Forschungszentrum Karlsruhe
Technik und Umwelt
Wissenschaftliche Berichte
FZKA 5909

ITER ECRF Window Block Design

– Final Report –

M. Thumm, O. Braz, R. Heidinger, S. Henry, A. Hofmann, M. Makowski, G. Soudée

Institut für Technische Physik
Institut für Materialforschung
Projekt Kernfusion

Mai 1997

Forschungszentrum Karlsruhe
Technik und Umwelt

Wissenschaftliche Berichte
FZKA 5909

ITER ECRF WINDOW BLOCK DESIGN

- Final Report -

M. Thumm, O. Braz, R. Heidinger, S. Henry,
A. Hofmann, M. Makowski*, G. Soudée

Institut für Technische Physik
Institut für Materialforschung
Projekt Kernfusion

*ITER Joint Work Site, Max-Planck-Institut für Plasmaphysik, Garching bei München

Forschungszentrum Karlsruhe GmbH, Karlsruhe
1997

Forschungszentrum Karlsruhe GmbH
Postfach 3640, 76021 Karlsruhe

ISSN 0947-8620

ITER ECRF FENSTER BLOCK DESIGN

- Schlußbericht -

Task No.: G 52 TD 06
ID No.: D 321

Kurzfassung

Der für ITER vorgeschlagene Fensterblock besteht aus einem flachen Array von Fenstereinheiten, jeweils zusammen mit einem Wartungs- und einem Isolationsvakuumschieber. Wir betrachten eine Hauptoption, die leicht 1 MW Dauerbetriebsleistung (CW) bei 170 GHz übertragen kann: Randgekühltes (Wasser, 293 K) Doppelscheibenfenster aus PACVD-Diamant in einem HE_{11}-Rillenhohlleiter mit 57,5 mm Innendurchmesser. Die Verwendung eines Doppelscheibenfensters mit Zwischenvakuum erlaubt einen einfachen Nachweis von Fensterfehlern (wie bei den JET LH und ICRH Systemen). Betrachtungen zur Bandbreite zeigen, daß der Scheibenabstand z. B. 52,9 mm = $30 \cdot \lambda$ sei sollte.

Bei einem Verlusttangens von $1{,}815 \cdot 10^{-5}$ beträgt die HF-Leistungsabsorption in einer Fensterscheibe ungefähr 400 W. Mit einem Wärmeübertragungskoeffizienten von 12 kW/m^2K zum Kühlwasser wird die Zentraltemperatur nicht höher als ungefähr 327 K und die Randtemperatur ca. 298 K sein. Die vorläufige Auslegung der Fenstereinheit und allgemeine Annahmen, Klassifizierungen, Richtlinien und Wartungsprozeduren werden in diesem Bericht vorgestellt.

Finite-Element (FE)-Berechnungen der mechanischen Spannungen, unter Mitberücksichtigung der Spannung an der Lötverbindung zeigen, daß der Hauptanteil der Von-Mises-Spannung genau an dieser Lötverbindung auftritt (314 MPa) und deswegen stets vorhanden ist. Im Falle eines Störfalles mit 0.5 MPa Überdruck würde die max. Spannung auf 348 MPa ansteigen und die Transmission von 1 MW Mikrowellenleistung würde die max. Von-Mises-Spannung vollends auf 375 MPa erhöhen. Alle diese Werte der mechanischen Spannung sind obere Grenzen, da eine starre Verbindung zwischen Lötkragen und Fensterscheibe angenommen wurde. Da die max. zulässige Biegespannung von PACVD-Diamant 600 MPa beträgt, sind alle Spannungen unterhalb der erlaubten Grenzen. In Zusammenarbeit mit der EU-Industrie wurden erfolgreich Metallisierungs- und Lötversuche mit kostengünstigen (grauen) Diamantscheiben von 25 mm bis 100 mm Durchmesser durchgeführt.

Außerdem wurden Auslegungsbetrachtungen für einen Fensterblock mit LNe (30 K) - randgekühlten Einscheibensaphirfenstern durchgeführt. Diese allerdings viel aufwendigere Option wird als Ersatzlösung betrachtet.

Ein Breitband-ECH-System mit stufenweise frequenzdurchstimmbaren Gyrotrons wird für das Plasma-Start-Up-System entwickelt und ein ähnliches System könnte auch für die Plasmaheizung und den Stromtrieb eingesetzt werden. Dabei werden zwei mögliche Lösungen eines Multifrequenz-Diamantfensters für Hochleistungsmillimeterwellen betrachtet: Multibandpass- und Brewsterfenster. Erste erfolgreiche Experimente am FZK mit einem Gyrotron, das mit einem konventionellen Resonator und einem Quarzglas-Brewsterfenster ausgestattet ist (Pulslänge 1 ms), ergaben 1 MW Ausgangsleistung für eine Serie von Resonatormoden im Frequenzbereich von 114 bis 166 GHz.

ITER ECRF WINDOW BLOCK DESIGN
- Final Report -

Task No.: G 52 TD 06
ID No.: D 321

Abstract

The proposed ITER window block consists of a flat array of window assemblies together with the maintenance and the isolation vacuum valves. We are considering one major option that can easily carry 1 MW CW power at 170 GHz: Edge-cooled (water, 293 K) twin PACVD-diamond window in a corrugated HE_{11} waveguide with 57.5 mm inner diameter. Through the use of a double window with an intermediate vacuum, window failures can be easily detected (as on the JET LH and ICRH systems).

For a loss tangent of $1.815 \cdot 10^{-5}$ the rf-power absorption in one window disk is approximately 400 W. With a heat transfer coefficient of 12 kW/m²K to the cooling the central window temperature will not be higher than approx. 327 K and the edge temperature is about 298 K. The pre-design of the window assembly and general assumptions, classifications, guidelines and procedures for the maintenance are presented in this report.

Finite element (FE) stress calculations including brazing/bonding stress show that the main Von Mises stress is at the window brazing (314 MPa) and is always present. During a 0.5 MPa overpressure event the max. stress increases to 348 MPa and the transmission of 1 MW microwave power finally increases the max. Von Mises stress to 375 MPa. All these stress values are upper limits since a rigid connection between brazing collar and window disk was assumed. Because the ultimate bending strength of PACVD diamond is 600 MPa all stresses are below the admissible limits. In collaboration with EU Industry metallization and brazing tests on cheap (gray) diamond samples with 25 mm to 100 mm diameter have been successfully performed.

Design considerations for a window block employing LNe (30 K) edge-cooled single-disk sapphire windows are also presented. This much more complicated option is kept as back-up solution.

A broadband ECH system employing step-tunable gyrotrons is being developed for the start-up system and a similar system could also be considered for heating and current drive. Two possible solutions for multi-frequency high-power millimeter wave diamond windows are considered: multi-pass-band window and Brewster window. First successful experiments at FZK with a conventional cavity gyrotron equipped with a fused quartz Brewster window (pulse duration 1 ms) gave 1 MW output power for all operating mode series in the frequency range from 114 to 166 GHz.

Contents

Executive Summary

The proposed ITER window block consists of a flat array of window assemblies together with the maintenance and the isolation vacuum valves. We are considering one major option that can easily carry 1 MW CW power at 170 GHz: Edge-cooled (water, 293 K) twin PACVD-diamond window in a corrugated HE_{11} waveguide with 57.5 mm inner diameter. Through the use of a double window, window failures can be easily detected (as on the JET LH and ICRH systems). A very high vacuum ($\approx 10^{-7}$ Pa) can be achieved within the interspace between the two window disks. Since the total volume is small, vacuum pumping can be done with only one Vac-Ion pump. Any failure of either window is detectable as a pressure rise on the ion pump even in the case in which a lower grade vacuum ($\approx 10^{-3}$ Pa) is present on the opposing surfaces. Bandwidth calculations show, that the disk distance should be e.g. 52.9 mm = 30 λ. Up to now there exist no measurements of tritium permeation through PACVD diamond.

For a loss tangent of $1.815 \cdot 10^{-5}$ the rf-power absorption in one window disk is approximately 400 W. With a heat transfer coefficient of 12 kW/m²K to the cooling water (flow velocity = 3m/s) the central window temperature will not be higher than approx. 327 K and the edge temperature is about 298 K. The pre-design of the window assembly and general assumptions, classifications, guidelines and procedures for the maintenance are presented in this report.

Finite element (FE) stress calculations including brazing/bonding stress show that the main Von Mises stress is at the window brazing (314 MPa) and is always present. During a 0.5 MPa overpressure event the max. stress increases to 348 MPa and the transmission of 1 MW microwave power finally increases the max. Von Mises stress to 375 MPa. All these stress values are upper limits since a rigid connection between brazing collar and window disk was assumed. Because the ultimate bending strength of PACVD diamond is 600 MPa all stresses are below the admissible limits.

In collaboration with EU Industry metallization and brazing tests on cheap (gray) diamond samples with 25 mm to 100 mm diameter have been successfully performed.

Design considerations for a window block employing LNe (30 K) edge-cooled single-disk sapphire windows are also presented. This much more complicated option is kept as back-up solution.

A broadband ECH system employing step-tunable gyrotrons is being developed for the start-up system and a similar system could also be considered for heating and current drive. Two possible solutions for multi-frequency high-power millimeter wave diamond windows are considered: multi-pass-band window and Brewster window. First successful experiments at FZK with a conventional cavity gyrotron equipped with a fused quartz Brewster window (pulse duration 1 ms) gave 1 MW output power for all operating mode series in the frequency range from 114 to 166 GHz (frequency tuning in 3.7 GHz steps by variation of the magnetic field in the cavity).

1. Introduction

Electron Cyclotron Heating (ECH) is one of the major candidates for Heating and Current Drive (H&CD) on ITER (170 GHz). ECH is extremely attractive from a reactor engineering point of view, offering compact launch structures, high injected power density, and a simple interface with the shield/blanket. High unit power, in excess of 1 MW, and high-efficiency gyrotrons significantly reduce the system cost by reducing the size of the auxiliary support systems (power supplies, cooling, input power, ...). CW operation is required for some of the anticipated ITER applications: 3s for start-up, 100 s for heating to ignition and 100-1000 s for current drive. In order for the Electron Cyclotron System to perform these functions a window must be developed to serve as both the tritium containment barrier on the torus and as the output window on the gyrotron. The former application is technically more demanding because a torus window must also serve as a reliable confinement barrier, should not use FC-cooling liquid, must not degrade unacceptably under modest neutron and γ irradiation (and X-rays) and in the case of cryo-cooling must be prevented by a cold trap from cryo-pumping. Part of the safety function is that it withstand a 0.5 MPa static pressure during off-normal events. The objective of the present research activity is to develop a torus window block design and specification.

The ECH system layout with the new beam launchers [1] applies the concept of the large feed through: no cuts of nuclear containments during the disassembly of the antenna, minimized shielding and respect of the cryostat as secondary barrier. Two mirrors are applied only in a dog leg behind the blanket and are also used to steer the beam (Figs. 1.1 and 1.2). Other mirrors are located outside the cryostat, where there is direct access for the maintenance. Four subparts are foreseen: the blanket plug, the shielding mirror block, the vessel feedthrough, the cryostat flange. The blanket plug is provided of seven horizontal window slots for the beams, it is installed separately and has its own cooling pipe both for bulk and the first wall. The shielding block is mounted inside the port duct behind the blanket plug to stop the neutron and γ-radiation streaming to the windows. It holds the mirrors, both the fixed and the steering ones. The ECH antenna is fixed on the vessel and the waveguides need compliance only towards the cryostat. This mirror shielding block is handled and installed separately on the vessel because its weight is above ten tons.

The big feed through is formed by the waveguides welded to the vacuum vessel flange and extended up to the cryostat, it includes two gate valves and the vacuum window. At the cryostat fluxes of neutrons and gammas will be several others of magnitudes lower than in the mirror region. This concept is consistent with full hands-on maintenance and with radiation limits of window materials.

A recess in the vessel flange up the back of the mirror block increases the radius of curvature of the waveguides under the imposed horizontal displacement. The flexible extension of the waveguides and the vacuum windows with their valves are supported by a frame, whose connection can be switched to the vessel flange, during assembly and for the transport or to the cryostat, during the operation. The present ECH layout provides room for 7 arrows of 8 beams suited both for plasma heating and current startup. A relevant problem of the design of the system is the double compliance between the blanket and the vessel and between the vessel and the cryostat. The relative transverse displacements for the case of worst combination of off-normal are up to 50 mm.

From the viewpoint for the realization of 1 MW CW operation, essentially all components of present-day transmission lines have been developed with the exception of the mm-wave window. In present ECH systems, edge-cooled (water) single-disk BN and fused quartz windows (EU,RF) as well as surface-cooled (FC-75) double disk sapphire windows (JA, US) are in use in pulsed operation at lower power levels. Water edge-cooled single-disk diamond windows (EU, JA), cryogenically edge-cooled single disk sapphire windows (EU, JA, RF) [2-12] and distributed windows (US)[13] are under test.

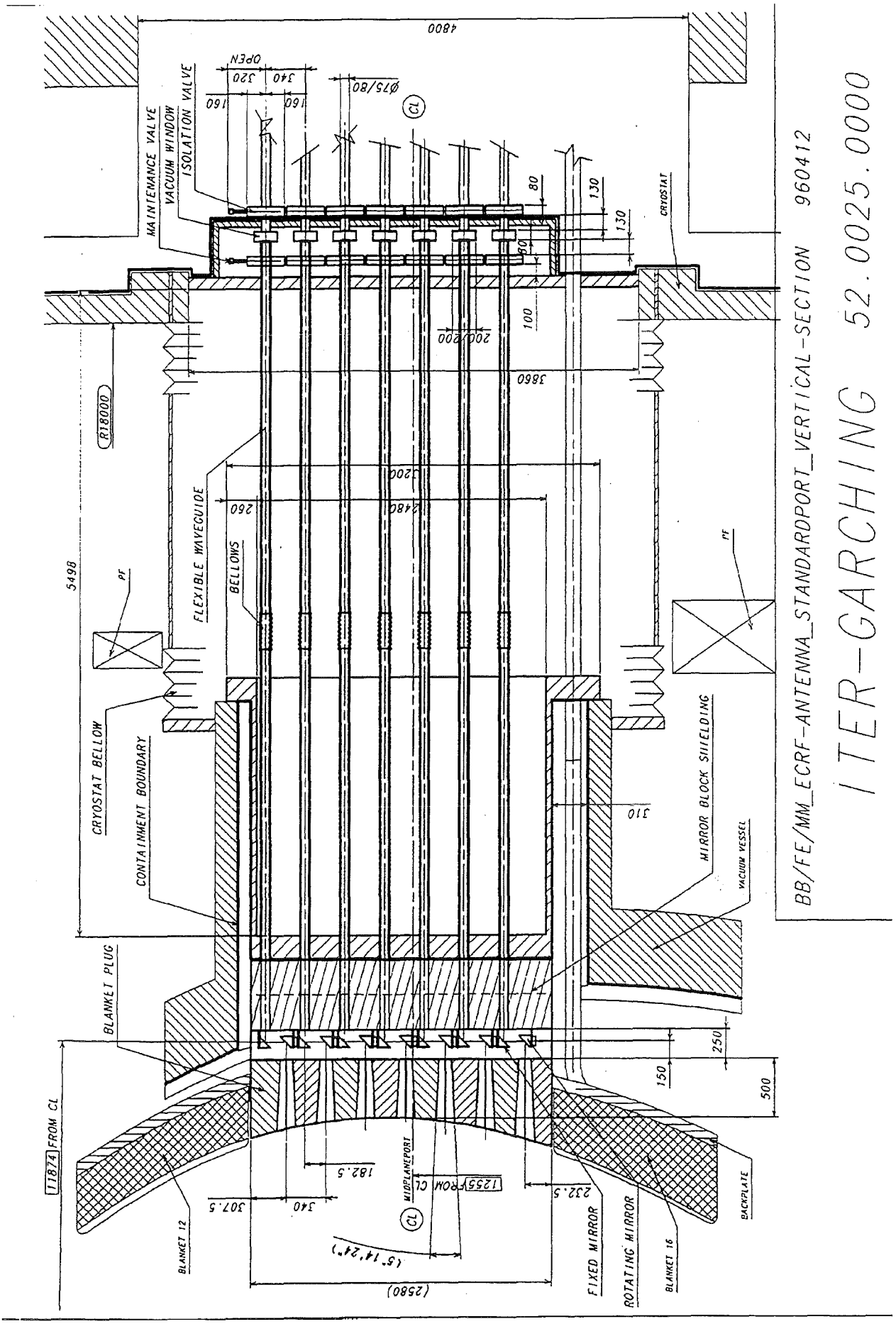

Fig. 1.1: Side view of the ITER-ECH antenna port. Dimensions relate to room temperature.

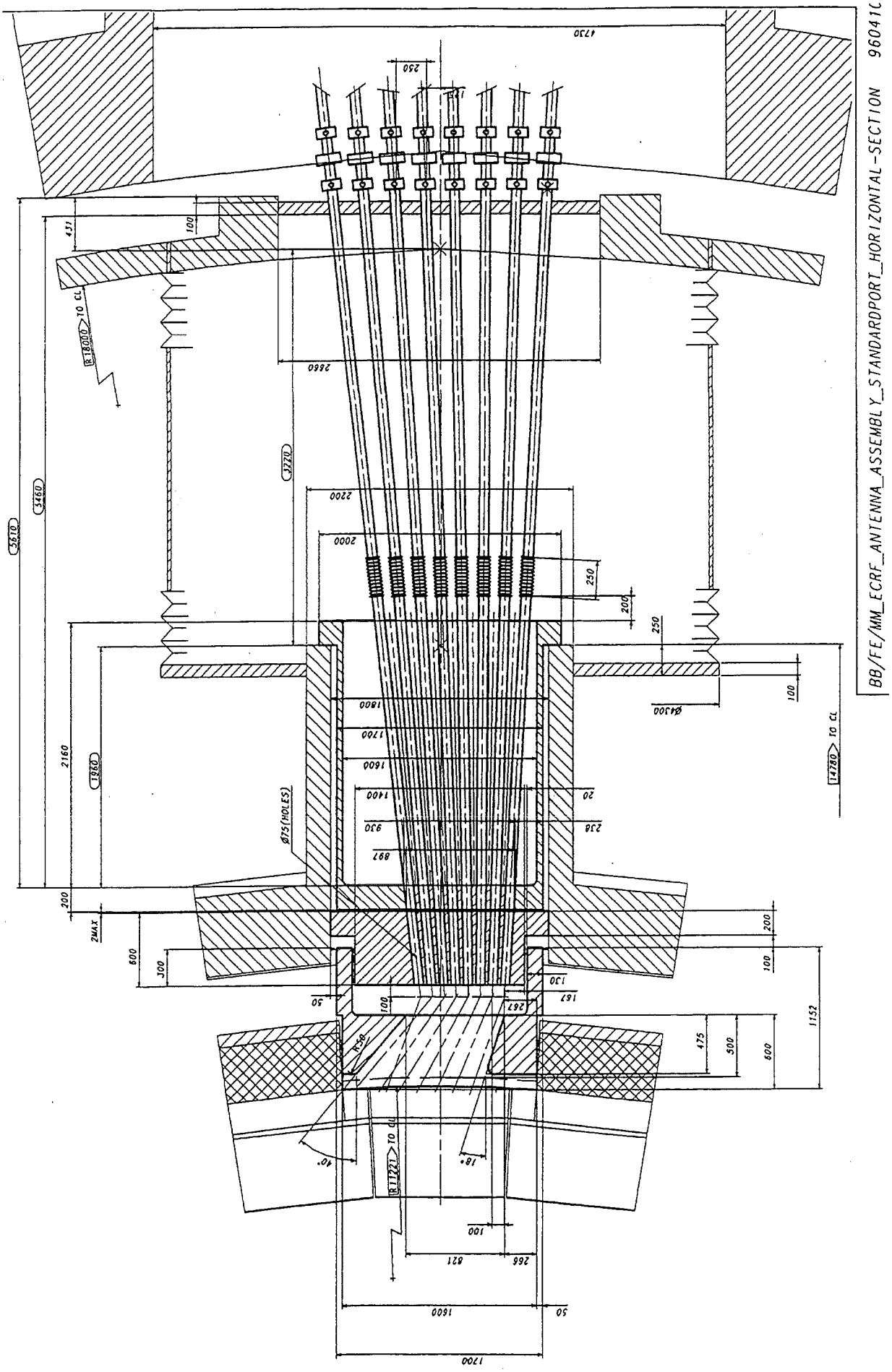

Fig. 1.2: Top view of the ITER-ECH antenna port. Dimensions relate to room temperature.

The present experimental state-of-the-art is summarized in Table I. As can be seen, no windows for CW applications at the MW power level exist.

Material	Type	Power (kW)	Frequency (GHz)	Pulse Length (s)	Institution
water-free fused silica	single disk inertially cooled	200	60	5.0	UKAEA/Culham
boron nitride	single disk water edge cooled	930	110	2.0	GYCOM (TORIY)
		550	140	3.0	GYCOM (TORIY)
		650	140	2.0	GYCOM (SALUT)
sapphire	single disk LN_2 edge cooled	530	118	5.0	CEA/CRPP/FZK/ THOMSON
		285*	140	3.0	IAP/INFK
		500	140	0.5	FZK/IAP/IPF/IPP
		370	140	1.3	FZK/IAP/IPF/IPP
sapphire	single disk with Cu anchor LHe edge cooled	410	110	1.0	JAERI/TOSHIBA
sapphire	double disk FC75 face cooled	200	60	CW	CPI
		400	84	10.5	NIFS/CPI
		350	110	10.0	CPI
		350	110	5.0	JAERI/TOSHIBA
		200	140	CW	CPI
		500	170	0.6	JAERI/TOSHIBA
sapphire	distributed water cooled	65**	110	0.3	GA/JAERI
		200*	110	0.7	GA/CPI
diamond	single-disk water edge cooled	300**	110	1	CPI/FOM
		50	110	CW	CPI/FOM

Note: * and ** indicates that the power density corresponds to that of a 1 MW (*) and 0.8 MW (**)HE_{11} mode, respectively

Tab. I: Experimental parameters of high-power millimeter-wave vacuum windows.

Recent advances in the area of window development have been made with respect to diamond. Diamond disks made by means of plasma assisted chemical vapor deposition (PACVD) of sufficient diameter, thickness and purity are available with which a high-power long-pulse 170 GHz window can be fabricated.

Table II summarizes potential options for 1 MW, CW, 170 GHz operation. Options ① to ③ being water cooled, are preferred for their simplicity, in particular for use as a torus window.

	Material	Type	RF-Profile	Cross-Section	Cooling
①	Sapphire/Metal	distributed	flattened Gaussian	rectangular (100 mm x 100 mm)	internally water cooled (300 K) $\tan\delta = 2\text{-}5 \cdot 10^{-4}$, k = 40 W/mK
②	Diamond	single-disk	Gaussian	circular (Ø = 80 mm)	water edge cooled (300 K) $\tan\delta = 2 \cdot 10^{-5}$, k = 1900 W/mK
③	Diamond	single-disk Brewster	Gaussian	elliptical (150 mm x 63.5 mm)	water edge cooled (300 K) $\tan\delta = 2 \cdot 10^{-5}$, k = 1900 W/mK
④	Silicon Au-doped	single-disk	Gaussian	circular (Ø = 80 mm)	edge cooled (260 K), refrigerator $\tan\delta = 2.5 \cdot 10^{-6}$, k = 200 W/mK
⑤	Silicon Au-doped	single-disk	Gaussian	circular (Ø = 80 mm)	LN_2 edge cooled (77 K) $\tan\delta = 4 \cdot 10^{-6}$, k = 1500 W/mK
⑥	Sapphire	single disk	flattened Gaussian	elliptical (285 mm x 35 mm)	LN_2 edge cooled (77 K) $\tan\delta = 6.7 \cdot 10^{-6}$, k = 1000 W/mK
⑦	Sapphire	single disk	Gaussian	circular (Ø = 80 mm)	LNe or LHe edge cooled (27 K) $\tan\delta = 1.9 \cdot 10^{-6}$, k = 2000 W/mK

Note that the power capability of options ②, ③, ⑤ and ⑦ is even 2 MW.

Tab. II: Options for 1 MW, CW, 170 GHz ECH windows.

The ITER window block resides at the boundary between in-vessel and ex-vessel systems and consequently forms the containment boundary for the ECH systems. Its design must be consistent with the general ITER design principles and machine constraints (port size, vacuum, etc.) and should address the major interfaces involving:

(i) safety and shielding
- vacuum leak detection methodology
- it must withstand a static 0.5 MPa pressure
- it forms the primary tritium containment boundary
- both mechanical and microwave performance must not be severely degraded by neutron and γ-radiation

(ii) cooling
(iii) maintenance and remote handling.

The total radiated ECH power for H&CD and plasma startup shall be 50 MW and the antenna system shall use only one horizontal port. In order to limit the number of gyrotrons the unit power must not be less than 1 MW. This power also roughly corresponds to the limits of present day window technology [6]. Expecting a corrugated HE_{11}-waveguide transmission efficiency from the gyrotron to the antenna mirrors of approximately 90 % one needs 56 (7x8) waveguide runs. Thus the window block will contain 56 window units.

A straight waveguide will be deformed by the relative motion between the vacuum vessel and the cryostat. Radial motion is absorbed with a bellows section (Figs. 1.1 and 1.2). Next largest motion is toroidal rotation of the port relative to the cryostat. Mode conversion is minimized by proper choice of ℓ/a^2 (where ℓ is the length and a is the radius of the waveguide) and thus of the beat

wavelength between the propagating mode HE_{11} and parasitic modes. A difference in relative height is also automatically compensated by the above. The length of the straight antenna waveguide of approximately 6.7 m results in an optimal waveguide diameter of 57.5 mm. Tapering the waveguide, with low conversion to parasitic modes, to a different diameter results at a frequency of 170 GHz in a relatively large overall length. Therefore a circular 57.5 mm diameter window is preferred.

Four general classes of single-disk high-power CW capable windows are being developed:

(a) water-cooled distributed sapphire window (US)
(b) water-edge-cooled diamond window (EU, JA)
(c) 200 K - cryo-cooled Au-doped silicon window (RF)
(d) LNe- or LHe- cryo-cooled sapphire window (EU, JA, RF)

The disadvantages of the distributed window are its complicated mechanical structure and its polarization characteristics which requires that polarizing miter bends are used after the window. This is in contrast to the incentive to have as much as possible of the components train before the window.

According to the above distribution of ECH window R & D between the ITER partners this present design report considers the following two options for a torus window with a rim for edge-cooling:

(1) Edge-cooled, single-disk PACVD-diamond window (water, 293 K)
(2) Edge-cooled, single-disk sapphire cryo-window (LNe, 30 K).

2. Characterization of Window Materials

In order to define the appropriate concepts for the development of 1 MW, CW millimeter-wave torus windows one has to compare the thermophysical, mechanical and dielectrical parameters of possible window materials related to the load-failure resistance R' and the power transmission capacity P_T at different temperatures. The features of sapphire and PACVD-diamond at room temperature and cryo-temperatures are summarized in Tables III and IV, where

$$R' = k \cdot \sigma_B \cdot (1-\nu)/E \cdot \alpha$$

and

$$P_T = R' \rho \cdot c_p/((1 + \varepsilon_r') \cdot \tan\delta).$$

The LN_2-edge-cooled sapphire window of the European 118 GHz TTE gyrotron (0.5 MW, 210 s), that operates close to the allowable lower limits of these two parameters, has R'=130 and P_T=80. The comparison of R' and P_T for the two window materials clearly shows, that there is no chance to use an edge-cooled, single-disk sapphire window at room temperatures. Experiments at CPI in US and NIFS and JAERI in JA showed, that even a double-disk FC75-face cooled sapphire window has a CW-power limit around 0.3-0.4 MW.

The temperature dependence of the loss tangent of different diamond grades at 145 GHz are presented in Figures 2.1 and 2.2 together with sapphire (HEMEX´grade) and Au-doped, high resistivity (HR) silicon [14-16]. Figure 2.3 shows the temperature dependence of the permittivity of diamond compared to sapphire at 145 GHz. The temperature behaviour of the thermal conductivity and the thermal expansion is plotted in Figures 2.4 and 2.5, respectively. In the temperature range 200 - 360 K the loss tangent and the permittivity are practically constant. This is not the case for sapphire. The frequency dependence of the loss tangent for diamond and sapphire is proportional to $1/\sqrt{f}$ and f, respectively (Fig. 2.6).

Tab. III
Thermophysical, Mechanical and Dielectrical Parameters of Window Materials related to Thermal Load -Failure Resistance and Power Transmission Capacity of Edge-Cooled Windows at Room Temperature
(p.c.=poly-crystalline, s.c.=single-crystalline)

Material	Sapphire (Al_2O_3) s.c.	Diamond (PACVD) p.c.
Thermal Conductivity k [W/mK]	40	1900
Ultimate Bending Strength σ_B[MPa]	410	600
Poissons Number ν	0.22	0.1
Density ρ [g/cm³]	4.0	3.5
Specific Heat Capacity c_p [J/g K]	0.8	0.5
Young's Modulus E [GPa]	385	1050
Therm. Expans. Coeff. α [10^{-6}/K]	5.5	1.2
Permittivity (145 GHz) ε_r'	9.4	5.66
Loss Tangent (145 GHz) tanδ [10^{-5}]	20	2
Metallizing/Brazing	o.k.	o.k. (1000°C) vacuum
Possible Size ∅ [mm]	270	160
Cost	high	high
Failure Resistance R' $R' = k\sigma_B (1-\nu)/E\alpha$	6.0	815
RF-Power Capacity P_T $P_T = R'\rho c_P/((1+\varepsilon_r')\tan\delta)$	0.09	107
Radiation Sensitivity n(10^{20}-10^{21}n/m²) γ/X (0.75 Gy/s)	no no	no no

Tab. IV
Thermophysical, Mechanical and Dielectrical Parameters of Window Materials related to Thermal Load -Failure Resistance and Power Transmission Capacity of Edge-Cooled Windows at LN_2-Temperature - 77 K (LNe-Temperature - 30 K)
(p.c.=poly-crystalline, s.c.=single-crystalline)

Material	Sapphire (Al_2O_3) s.c.	Diamond (PACVD) p.c.
Thermal Conductivity k [W/mK]	900 (20000)	10000
Ultimate Bending Strength σ_B[MPa]	410	600
Poissons Number ν	0.22	0.1
Density ρ [g/cm³]	4.0	3.5
Specific Heat Capacity c_p [J/g K]	0.8	0.5
Young's Modulus E [GPa]	402 (405)	1050
Therm. Expans. Coeff. α [10^{-6}/K]	5.5	1.2
Permittivity (145 GHz) ε_r'	9.3	5.63
Loss Tangent (145 GHz) tanδ [10^{-5}]	0.57 (0.2)	1
Metallizing/Brazing	o.k.	o.k. (1000°C) vacuum
Possible Size ∅ [mm]	270	160
Cost	high	high
Failure Resistance R' $R' = k\sigma_B (1-\nu)/E\alpha$	130 (2871)	4286
RF-Power Capacity P_T $P_T = R'\rho c_P/((1+\varepsilon_r')\tan\delta)$	71 (4460)	1132
Radiation Sensitivity n($0.3 \cdot 10^{21}$n/m²)	no	
γ/X (0.75 Gy/s)	no	no

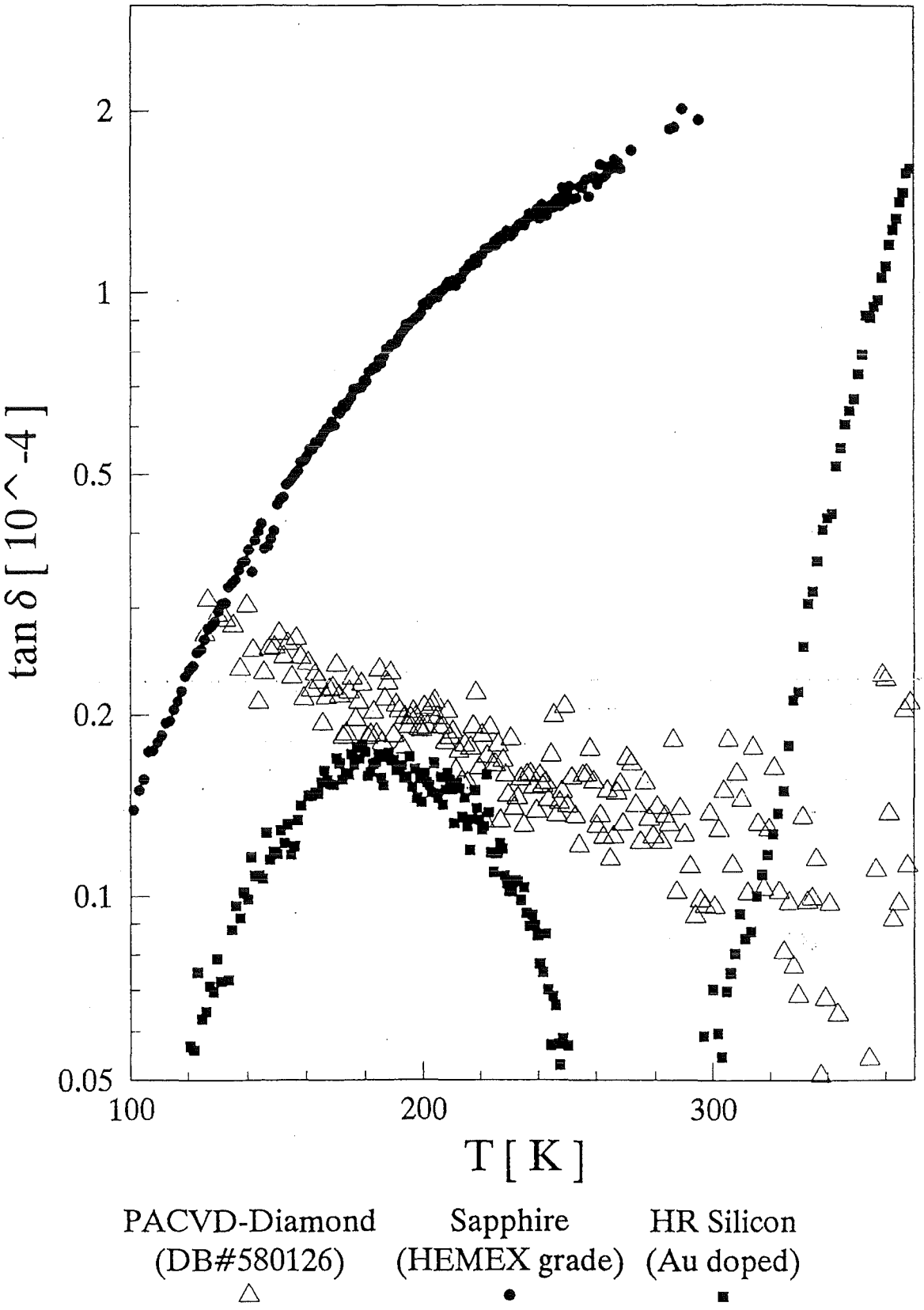

Fig. 2.1: Temperature dependence of dielectric loss of different high power mm-wave window materials at a frequency of 145 GHz.

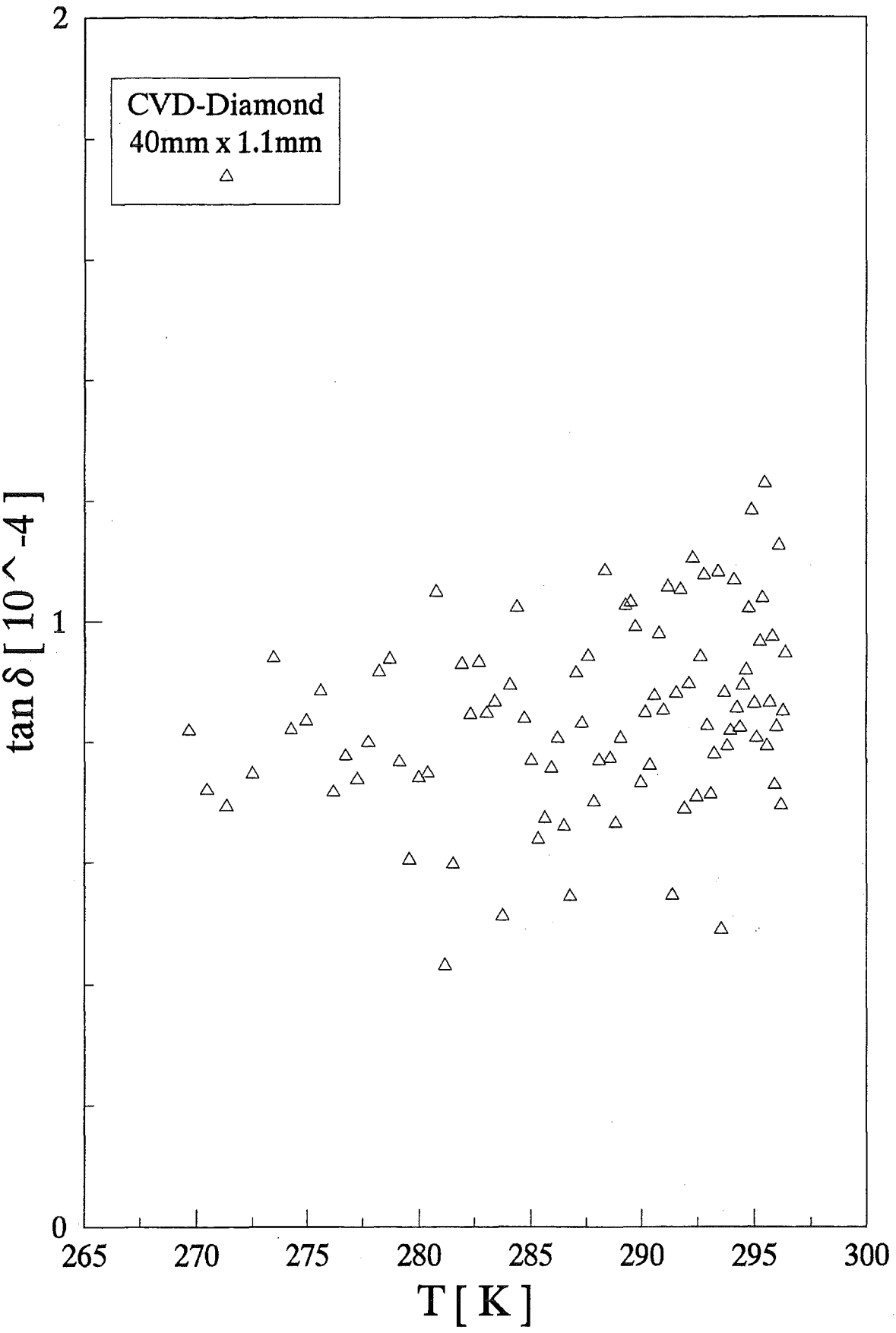

Fig. 2.2: Temperature dependence of dielectric loss of PACVD-diamond (diameter = 40 mm, thickness = 1.1 mm) at a frequency of 145 GHz.

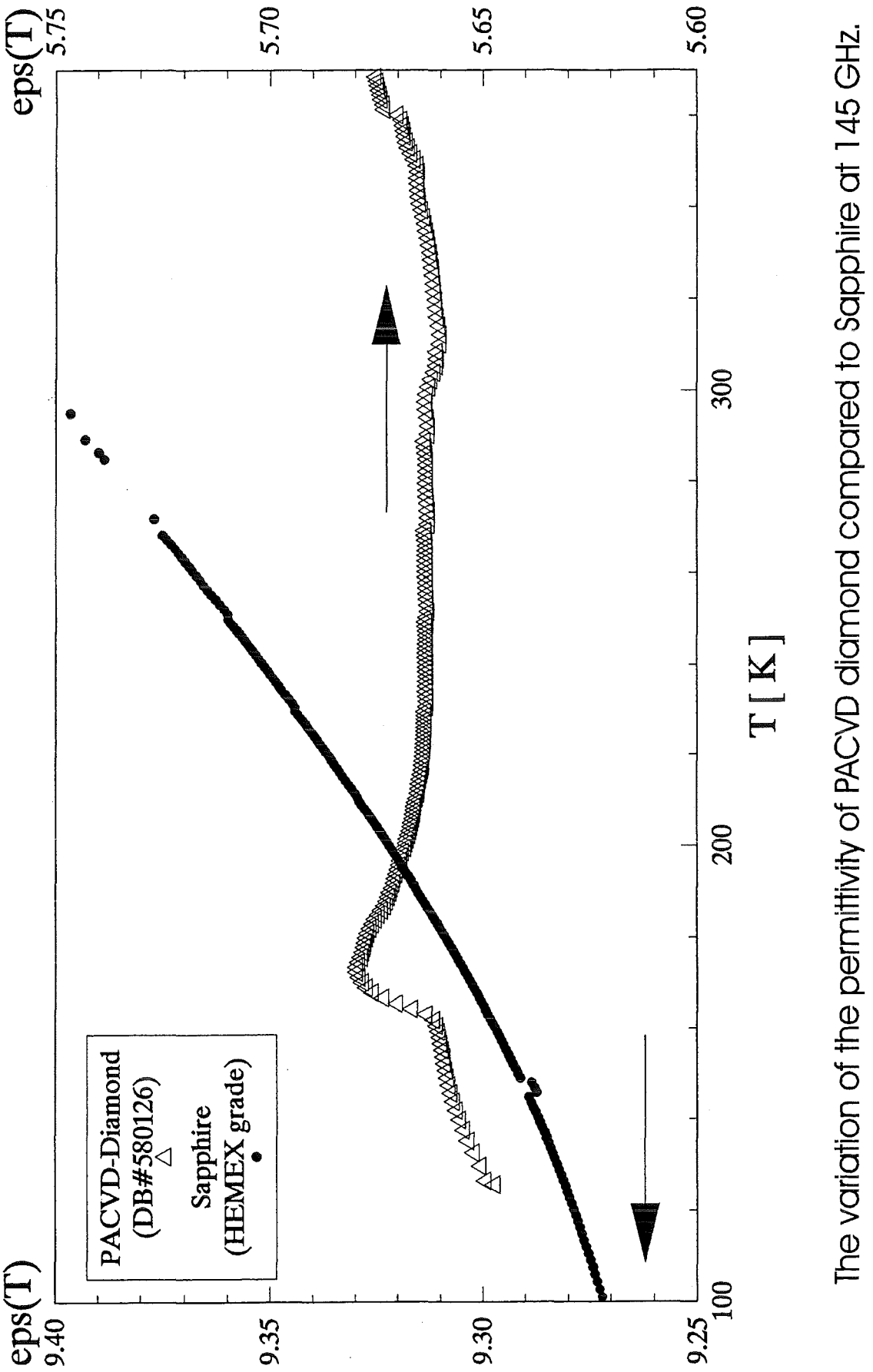

Fig. 2.3: Temperature dependence of permittivity of PACVD-diamond compared to sapphire at a frequency of 145 GHz.

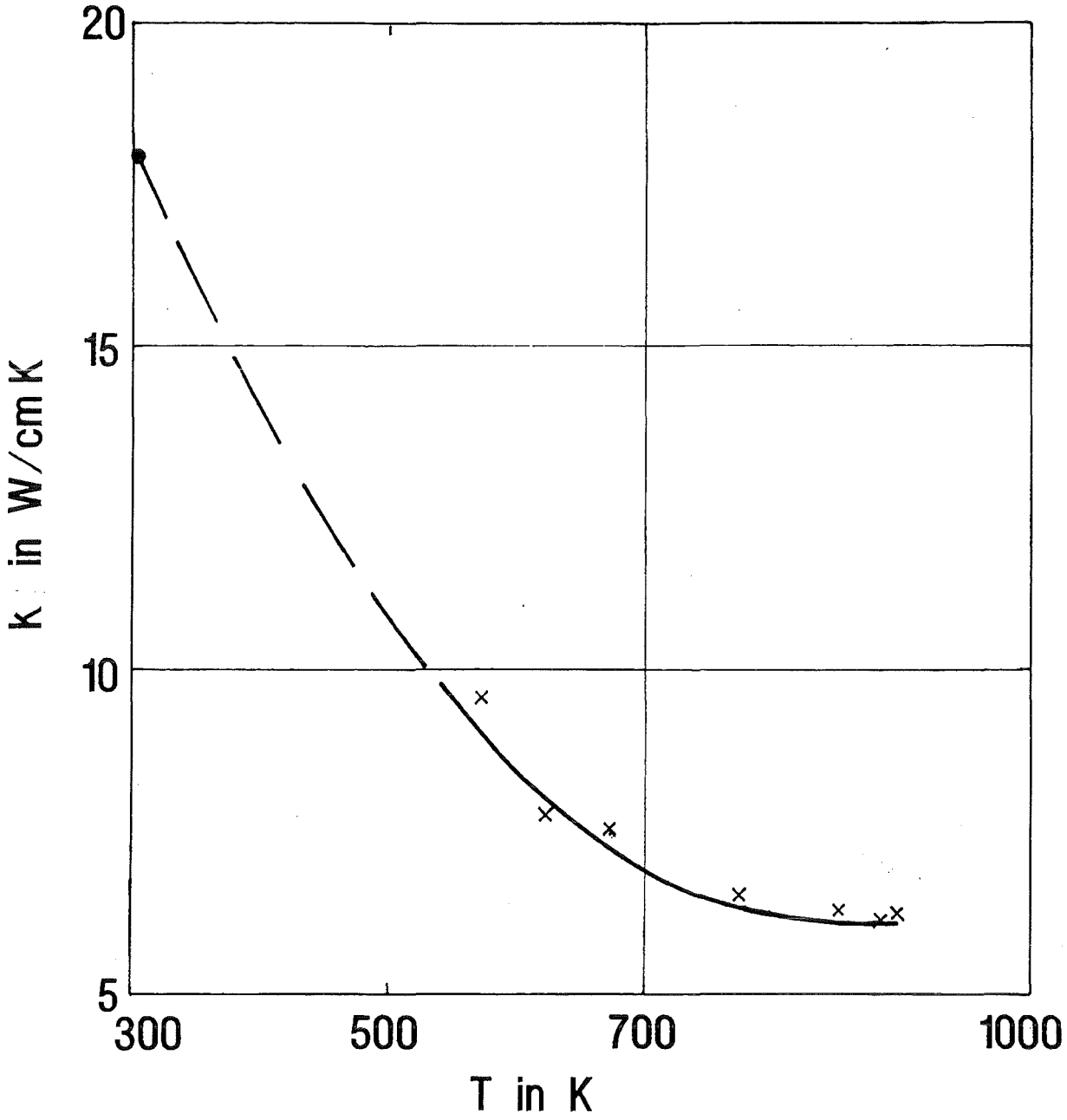

Fig. 2.4: Temperature dependence of thermal conductivity k of PACVD-diamond (B. Schulz and M. Rohde, FZK).

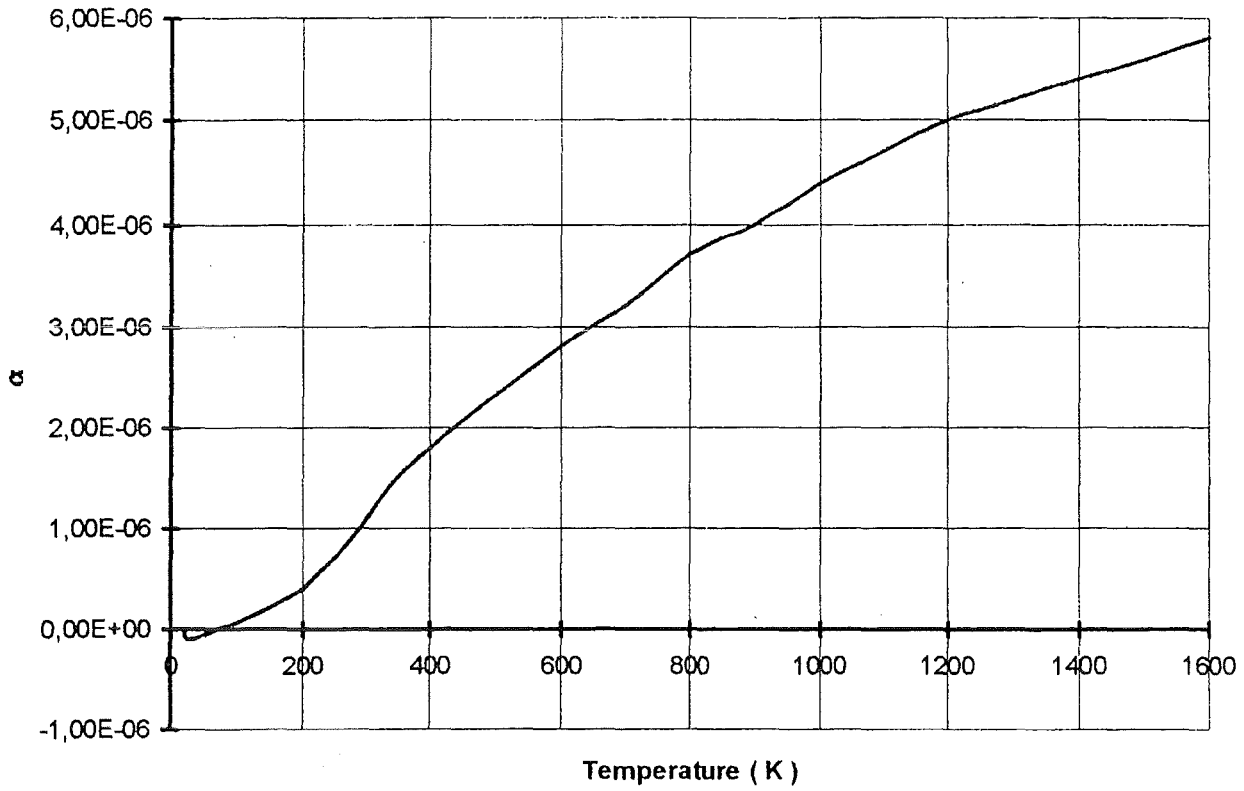

Fig. 2.5: Temperature dependence of thermal expansion coefficient α of diamond [17].

In order to check the usability of large-size PACVD-diamond disks for high-power millimeter-wave vacuum barrier windows at room temperature (T = 293 K) a first series of experiments, using a 170 GHz, 300kW, 200 ms JAERI/Toshiba gyrotron, have been performed. The dielectric loss tangent at a frequency of 170 GHz has been determined to be $\tan(\delta) = 1.3 \cdot 10^{-4}$. By comparing the experimental results to numerical simulations the thermal conductivity was estimated to be about $k \approx 1800$ W/mK. This preliminary results indicate that a single-disk PACVD diamond window assembly using a water-edge cooling could fulfill the requirements for a continuous wave (CW) transmission of millimeter wave power in the megawatt range.

HEMEX sapphire shows identical behavior of the loss tangent without and after neutron irradiation at 293 K (neutron energy > 0.1 MeV, neutron fluence 10^{21} n/m²) and 77 K ($0.3 \cdot 10^{21}$ n/m²) and there is no measureable in-beam effect (X-ray dose rate up to 0.75 Gy/s) for these neutron-irradiated HEMEX samples (Fig. 2.6). For diamond at 293 K for a neutron fluence of 10^{20} n/m² and at the highest X-ray dose rate tested, 3600 Gy/s, no measureable increase in loss is measured. This is most probably due to the high intrinsic defect content of the material.

Figure 2.7 shows the variation of the dielectric loss of PACVD-diamond under X-ray irradiation measured as a function of the tube current at 300 kV tube voltage. The results and scope of the FZK neutron irradiation projects are summarized in Table V.

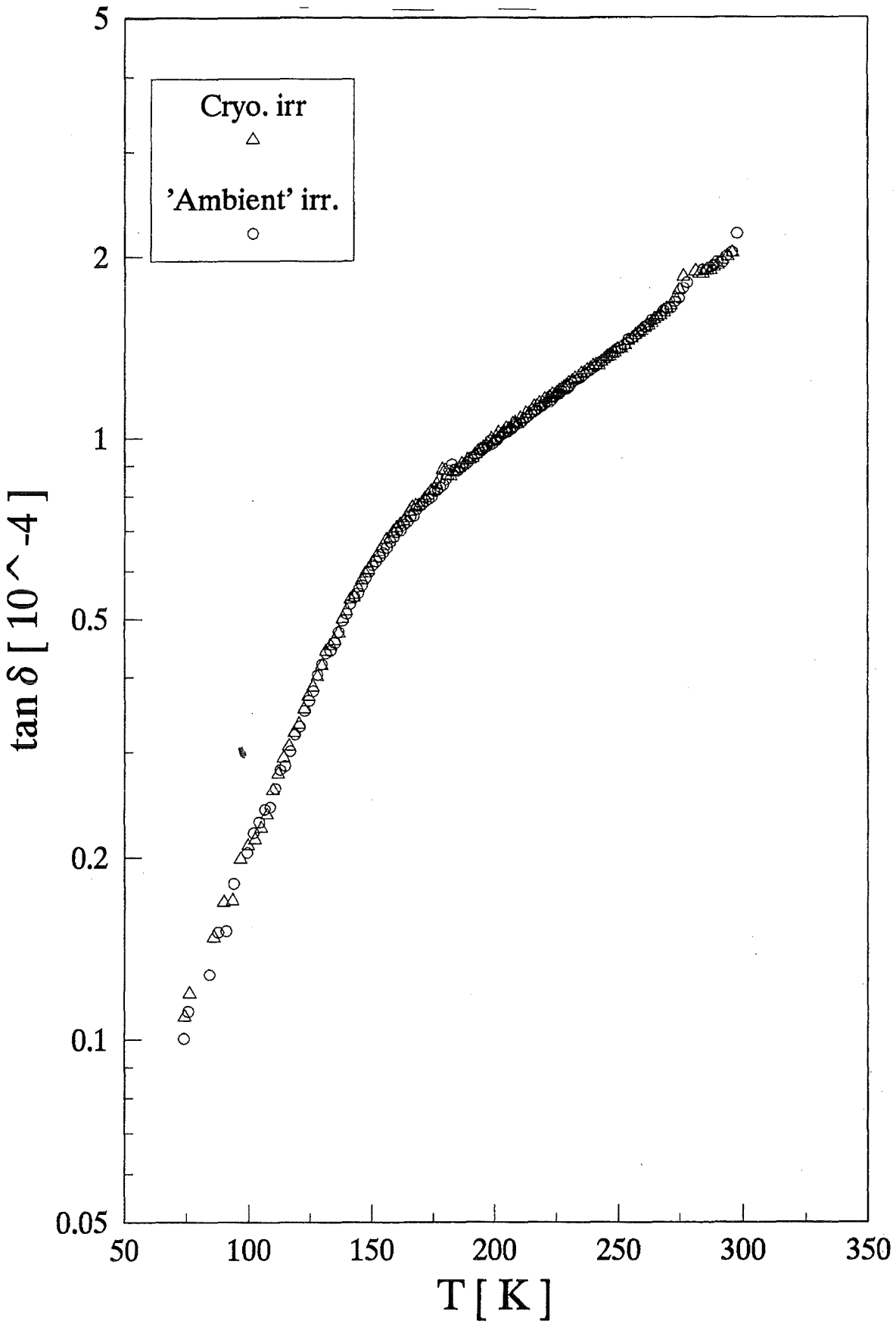

Fig. 2.6: Temperature dependence of the dielectric loss in HEMEX sapphire after neutron irradiation at room temperature (neutron fluence 10^{21} n/m²) and after irradiation at 77 K ($0.3 \cdot 10^{21}$ n/m²) measured at 145 GHz.

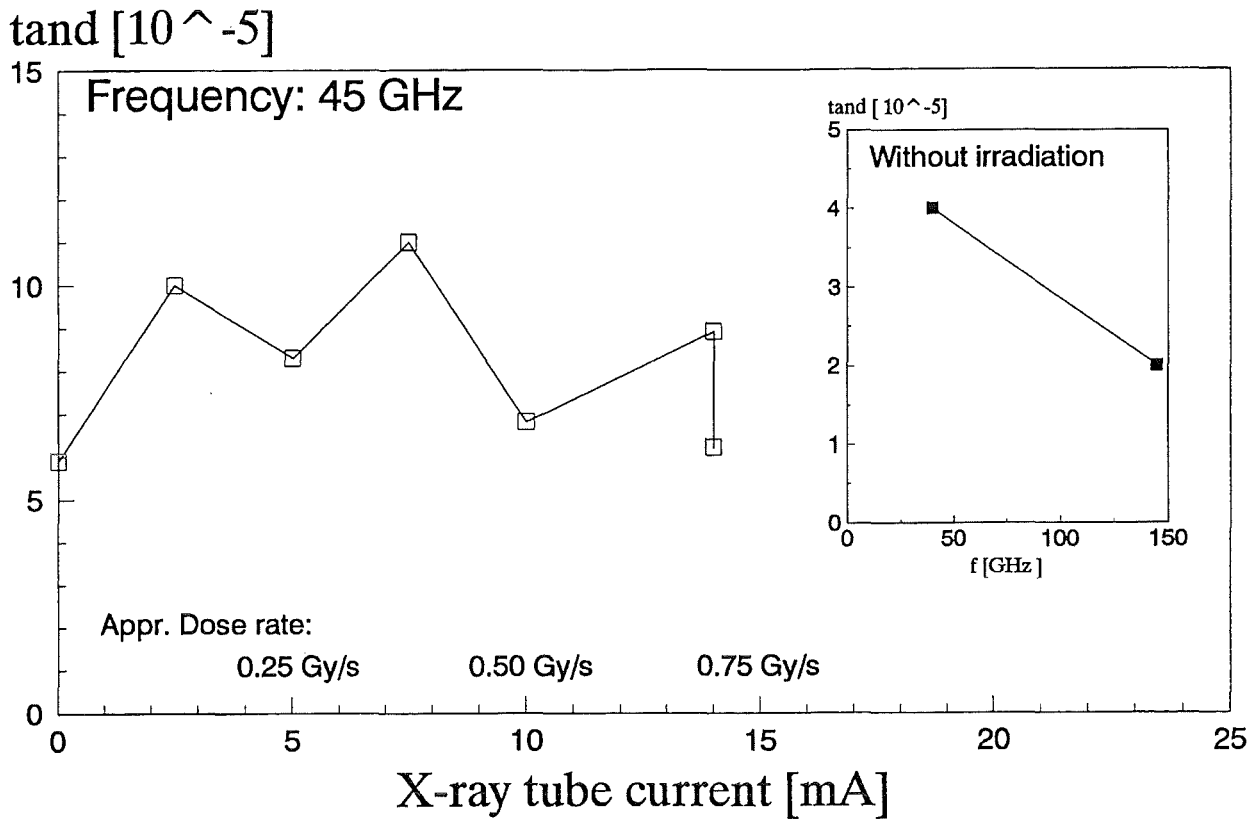

Fig. 2.7: Dielectric loss of PACVD-diamond under X-ray irradiation measured as a function of the dose rate [18]. Tube voltage 300 kV.

Type of irradiation	Dielectric specimens	Thermophys. specimens	T_{irr}	Fluence (E > 0.1 MeV)	Irradiation time	Status
Cryo I (Petten NL)	HEMEX U. C. Sapphire Quartz	as dielectric specimens	77 K	10^{21} n/m^2	2 - 3 days	Irradiation performed: July 1995 Specimens under study
Ambient I (Geesthacht, D)	CVD Diamond Doped Silicon Pure Silicon	as dielectric specimens	~ 330 K	10^{20} n/m^2	2 - 3 days	Irradiation peformed: November 1996 Specimens under study
Cryo II (Garching, D)	no specimens insufficient capsule size	U. C. Sapphire	4.2 K	10^{20}n/m^2	< 2 - 3 weeks	Irradiation performed: December 1996 Specimens under study
Ambient II (Geesthacht, D) or (Petten, NL)	as in Ambient I	as in Ambient I	~ 330 K	10^{21} - 10^{22} n/m^2	2 - 14 days	
Cryo III (Petten) (2nd choice)	HEMEX U.C. Sapphire (Doped Silicon)	as dielectric specimens	77 K	10^{19} - 10^{21} n/m^2	< 1 week	

Tabel V: Scope of the FZK neutron irradiation projects within the ITER/NET task 'PPM4' on 'Ceramics for Heating and Current Drive Systems' (1995 - 1997).

3. Permeation of Tritium through Window Materials

The permeation of tritium through mm-wave window materials is a so called gas driven permeation (GDP) of T_2 molecules. The molecules are adsorbed at the window disk surface, thus must be dissociated to tritium atoms which finally diffuse into the bulk material, resulting in comparatively low penetration efficiency. Form of window material (e.g. single-crystal, poly-crystalline, α-, β-, sintered) and impurity levels can have a large effect on the specimen permeability. The tritium diffusion coefficent of MgO-doped poly-crystalline Al_2O_3 is more than 3 orders of magnitude larger than for pure Al_2O_3. The difference in the diffusion coefficient of single-crystal α and β SiC is roughly 1 to ½ orders of magnitude. Up to now no measurements for PACVD diamond have been published. The measured permeation coefficients of ceramics for hydrogen are drastically lower than those for metals [19,20]. For example, at a temperature of 500 K, the permeation coefficient of alumina is, respectively, 10^{15}, 10^{18} and 10^{20} times lower than that of tungsten, gold and stainless steel. This means that probably the weakest element of the window for tritium permeation is the brazing/bonding collar and not the disk.

4. Edge-Cooled PACVD-Diamond Window

A water-cooled window has the two very important advantages, that it is employing a cheap and effective coolant and it is compact, simple and likely more reliable as other solutions and thus can be also easily used as torus window.

As a potential new material for non-cryogenically cooled high-power mm-wave windows, diamond is very attractive due to its outstanding mechanical strength properties, modest dielectric constant, relatively low loss and phenomenal thermal conductivity at room temperature. Current PACVD capabilities have allowed for tests with samples of up to 40 mm diameter and 1.1 mm thickness at f = 145 GHz [14]. Manufacturers (GEC-Marconi, DeBeers) claim, that they also can produce samples of up to 160 mm diameter. DeBeers company has already manufactured several disks of about 100 mm diameter and around 2 mm thickness. The current price of such a disk is 70000 - 90000 US$. The loss tangent values of these large diameter disks are approximately 10^{-4} with tendency to decrease, so that we consider a value of around $2 \cdot 10^{-5}$ as feasible in a relatively short time schedule.

Numerical calculations at 170 GHz (HE_{11} mode) on the temperature and stress distribution have been performed using the finite element code ABAQUS supported by the pre-processor code FEMGEN for preparation of the discretization mesh. The assumed window disk has a waveguide aperture of 57.5 mm diameter with a rim for water edge cooling at 293 K. The thickness is 1.852 mm ($5 \cdot \lambda/2$ in PACVD diamond). The 1%-reflection bandwidth is Δf = 2.3 GHz. The calculations use the temperature dependences of the diamond material parameters presented in section 3. The heat transfer coefficient to the cooling water is assumed to be 12 kW/m^{2}K (flow velocity = 3m/s).

4.1 Thermal Finite Element Calculations

Figure 4.1 shows the maximal (center) and minimal (edge) temperature of the diamond disk in dependence of the width of the cooling rim at a mm-wave power of 1 MW. As we can easily see, a cooling rim of about 10 mm width is sufficient to get a maximum center temperature of only around 327 K and an edge temperature of not more than 298 K. The corresponding time dependence is plotted in Fig. 4.2. The power absorbed in the disk is 400 W. Figure 4.3 presents the maximum and minimum temperatures in dependence of the transmitted power showing that the power capability is even higher than 1 MW.

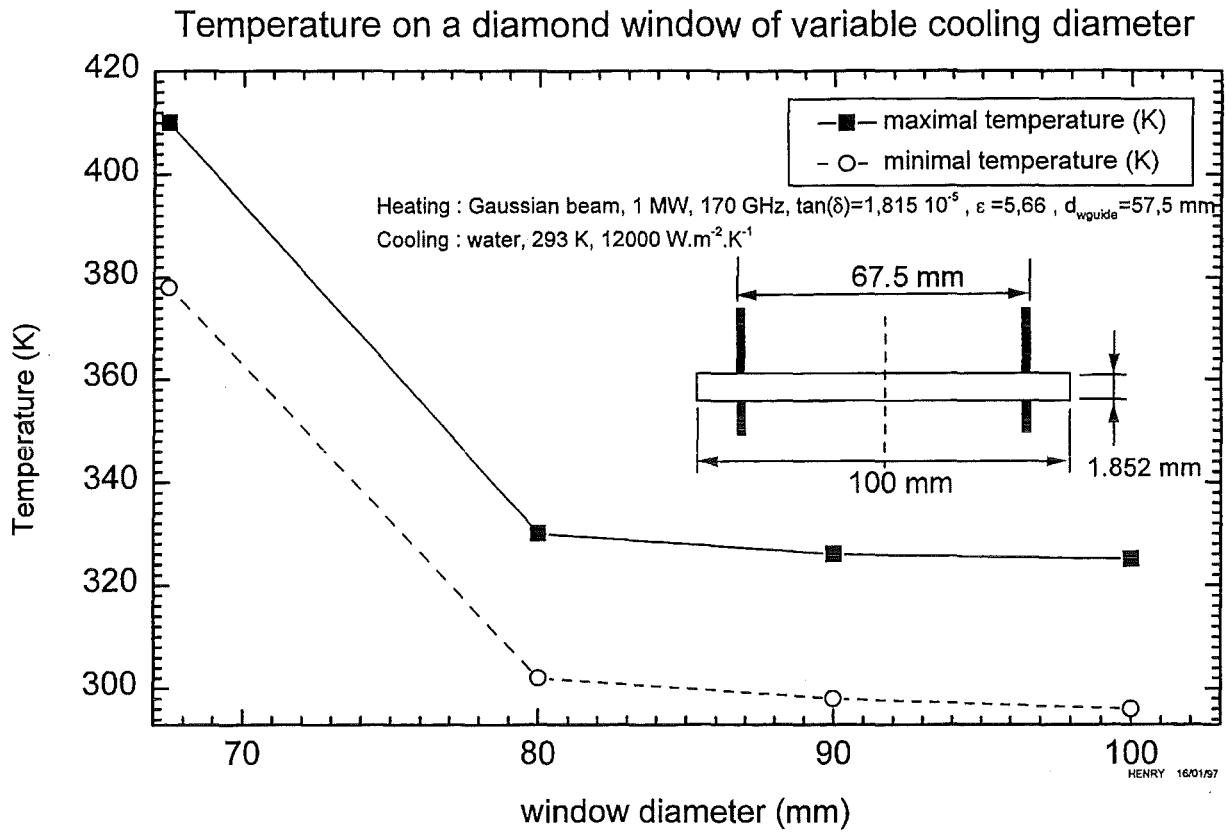

Fig. 4.1: Dependence of center and edge temperature of PACVD-diamond windows on the width of the applied cooling rim at 1 MW mm-wave power.

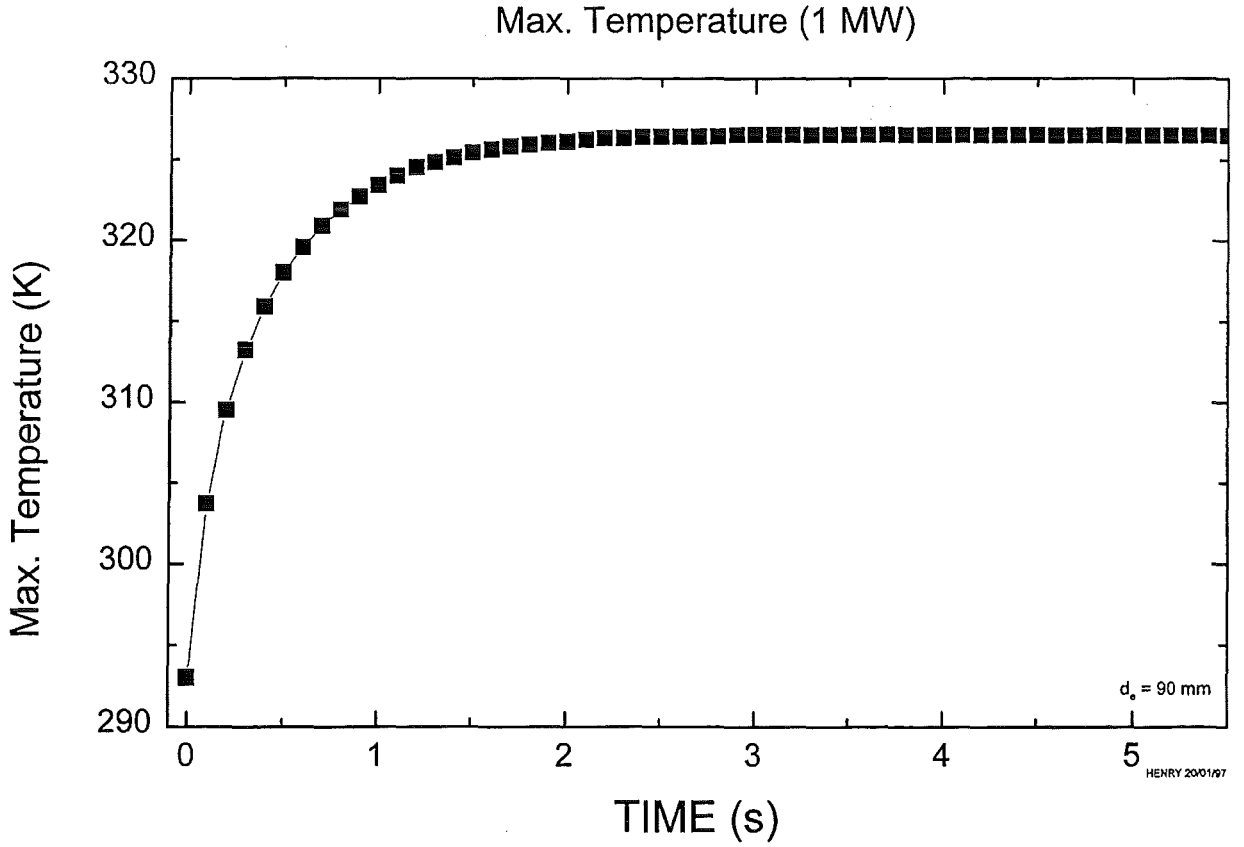

Fig 4.2: Time dependence of center temperature of PACVD-diamond windows at 1 MW.

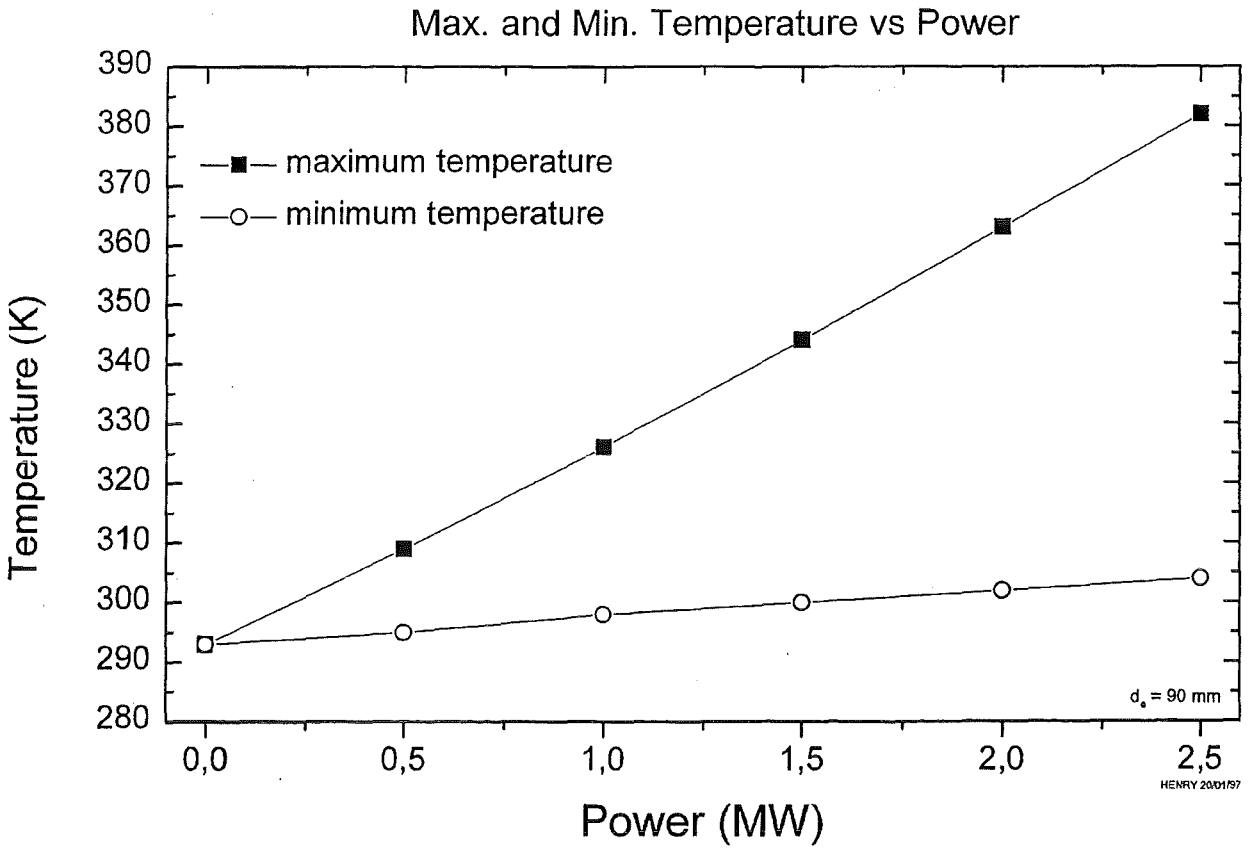

Fig. 4.3: Dependence of center and edge temperature of PACVD-diamond windows on the transmitted mm-wave power.

4.2 Finite Element Calculations on Stresses

Finite element (FE) stress calculations including brazing/bonding stress show that the dominant Von Mises stress arises from the differential thermal expansion when bonding diamond to molybdenum (314 MPa) and is always present. Molybdenum is chosen as metal because it has the lowest thermal expansion coefficient at high temperatures around 800 - 1000°C (5 - 6 µm/mm). During a 0.5 MPa static overpressure event the max. stress increases to 348 MPa and 1 MW transmitted mm-power finally increases the max. Von Mises stress to 375 MPa (Figs. 4.4 and 4.5). All these stress values are upper limits since a rigid connection between brazing collar and window disk was assumed. Because the ultimate bending strengh of PACVD-diamond is 600 MPa all stresses are below the admissible limits.

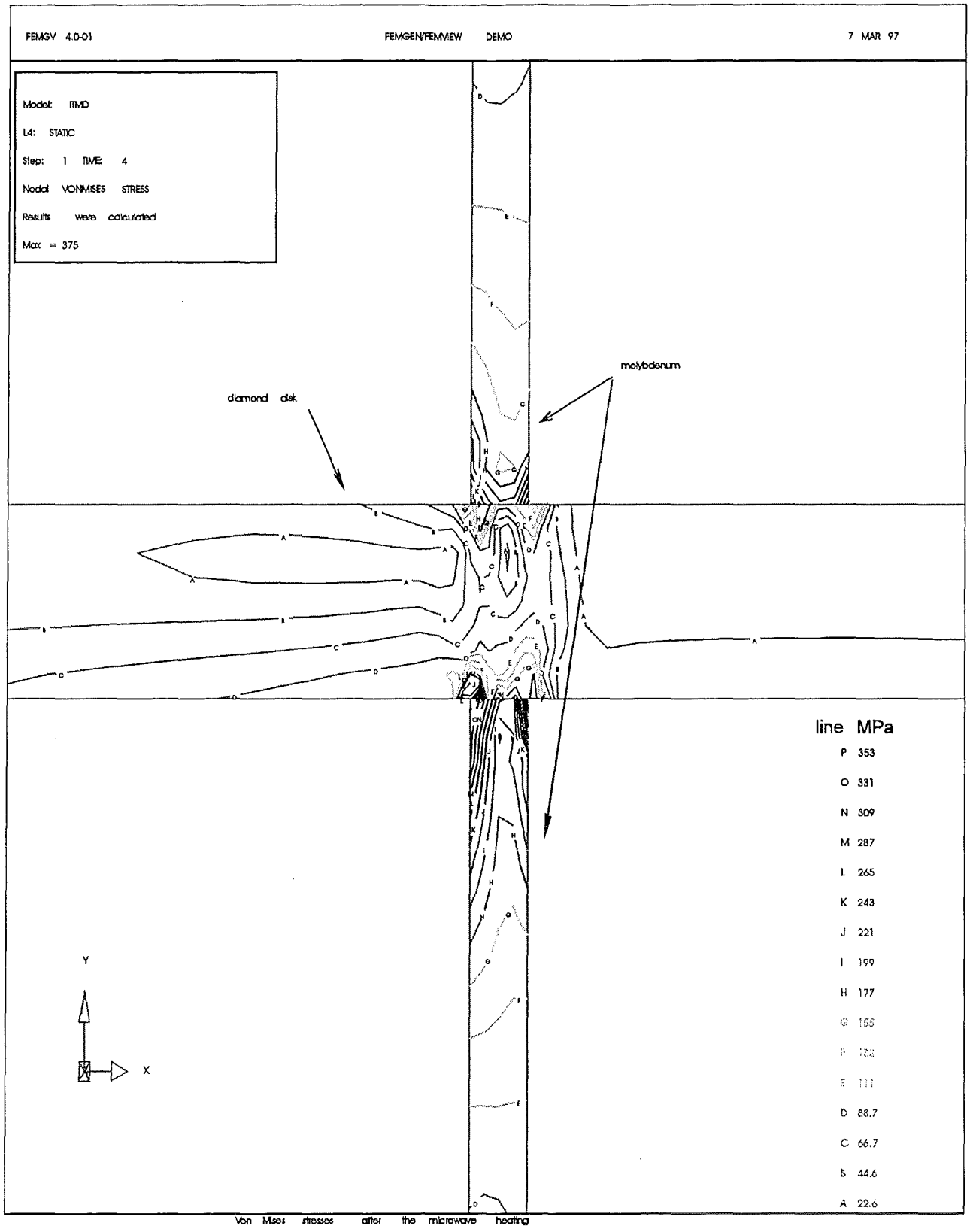

Fig. 4.4: Von Mises stresses during 1 MW operation at 0.5 MPa static overpressure.

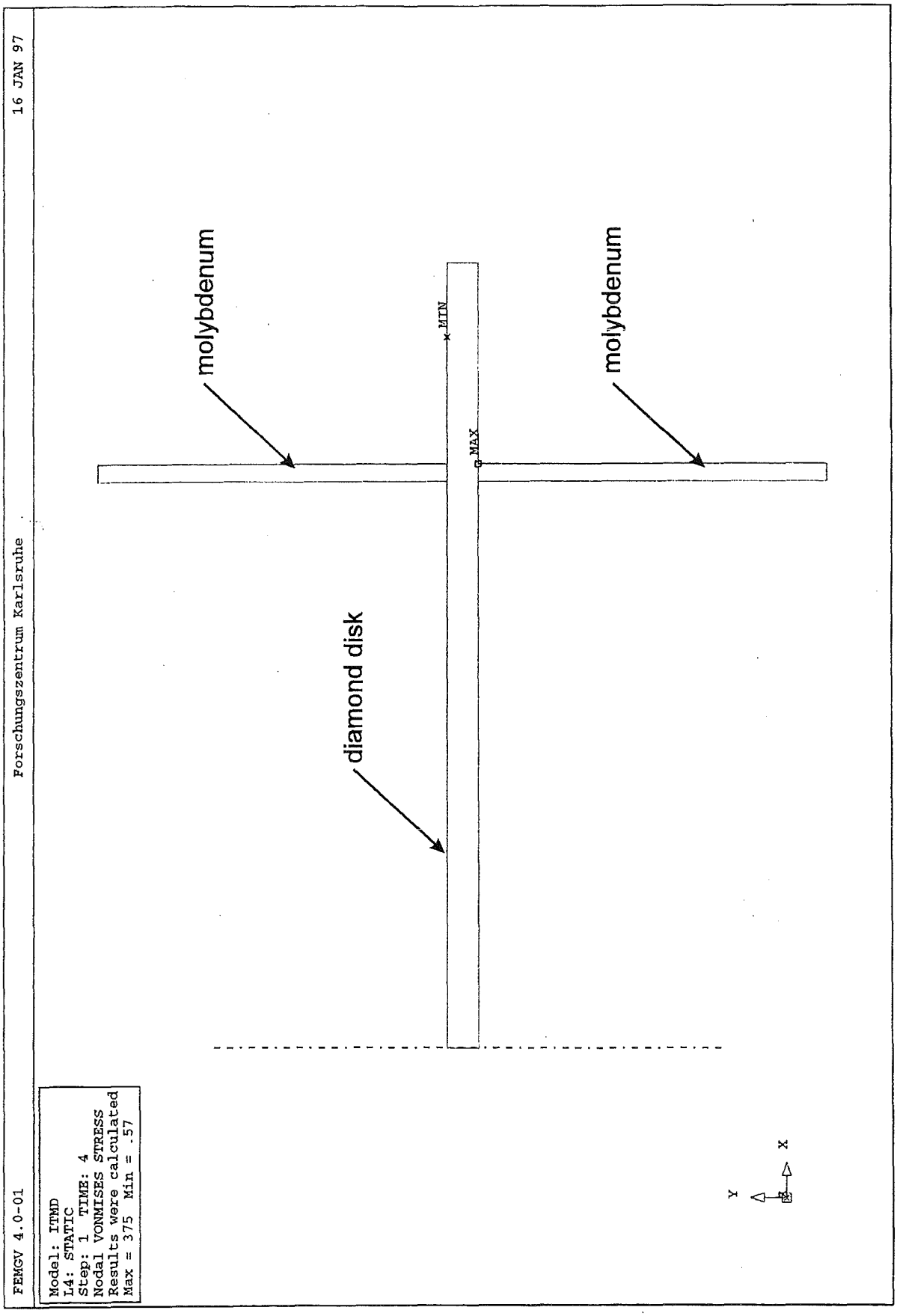

Fig. 4.5: Location of the maximum and the minimum Von Mises stresses during 1 MW operation at 0.5 MPa static overpressure.

In collaboration with EU Industry (DeBeers), FZK has performed thermomechanic cycling tests of two cheap (gray) diamond windows (48 mm diameter, 0.5 mm thickness) brazed to a molybdenum waveguide. The two window assemblies had the same construction but the diamond disks had non-polished and polished surfaces, respectively. The following thermocycle has been applied which is typical for bake out of gyrotrons:

heating to 240 °C in 7 hours, holding at 240 °C for 15 hours,
heating to 390 °C in 5 hours, holding at 390 °C for 7 hours,
heating to 480 °C in 3 hours, holding at 480 °C for 20 hours,
cooling to 370 °C in 4 hours, holding at 370 °C for 8 hours,
cooling to 20 °C in 24 hours.

After this cycle the 48 mm diameter window with the non-polished surface was still UHV tight and no diffusion degrading of the brazing has been observed (leak rate better than 10^{-9} mbar l/s), the window with the polished surface got a leak of the brazing (leak rate: 10^{-4} to 10^{-5} mbar l/s). The cause of the leak was probably a bad brazing. A recent test with a polished 100 mm diameter window (1 mm thickness) was also successful (Fig. 4.6).

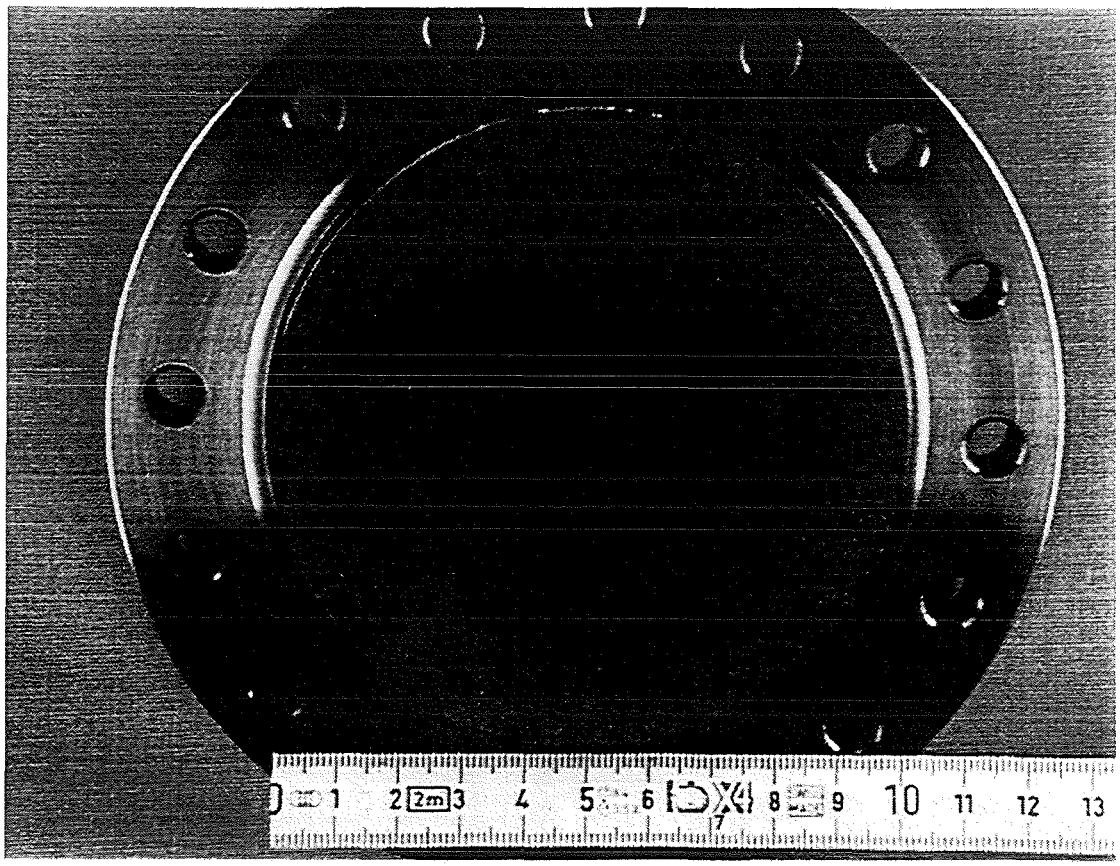

Fig. 4.6: Photograph of a 100 mm diameter diamond window assembly.

5. Design of Window Block

Figure 5.1 shows a schematic 3D-view of the ECH antenna system with the window block containing a flat 7x8 array of window assemblies (Fig. 5.2) consisting of the window unit and the maintenance and isolation valves. The dimensions of the window block are approximately 2.2 m x

2.5 cm x 0.7 m. The window block can be isolated from the vacuum vessel and removed without breaking vacuum.

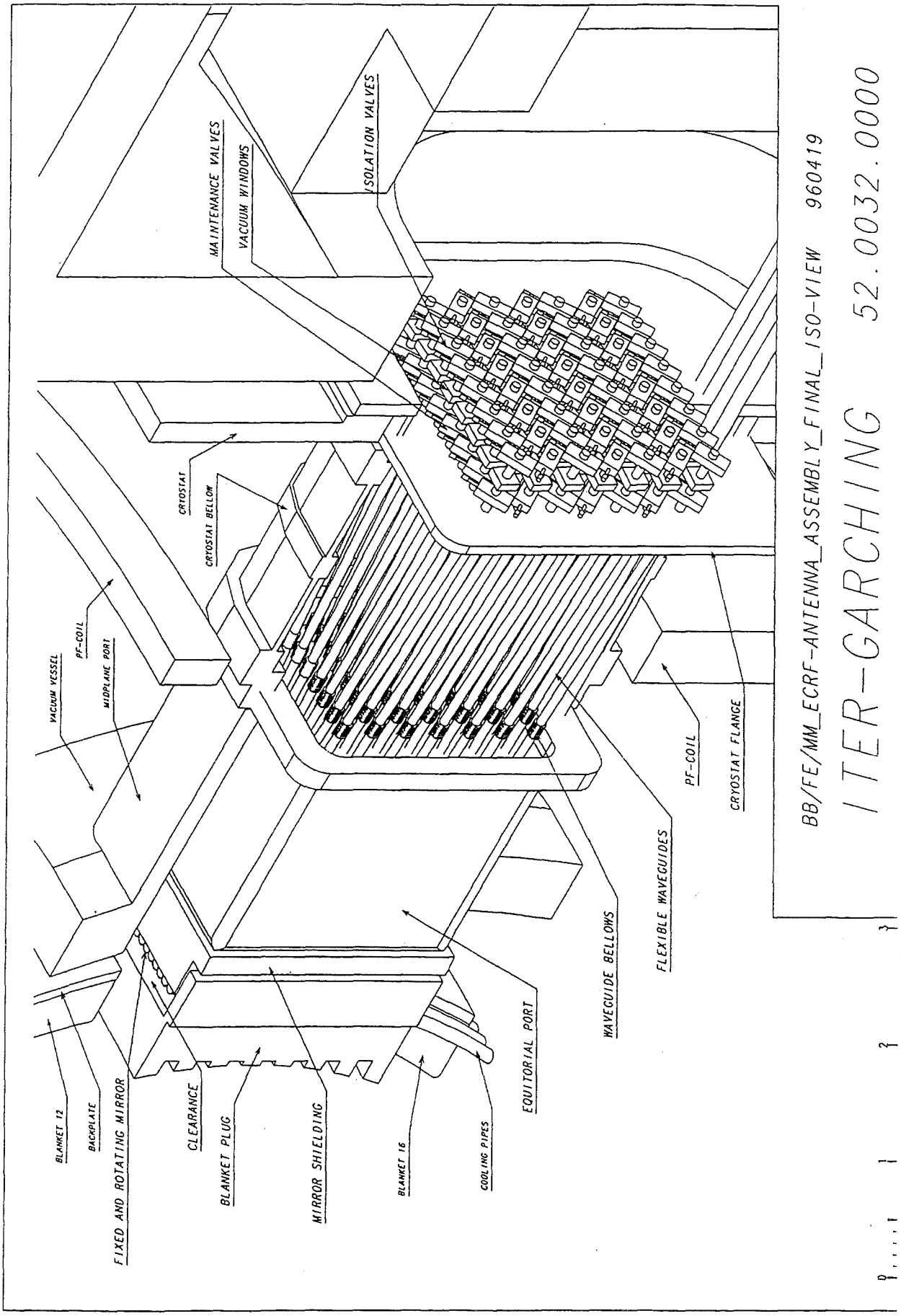

Fig. 5.1: Schematic 3D-view of the ECH antenna assembly.

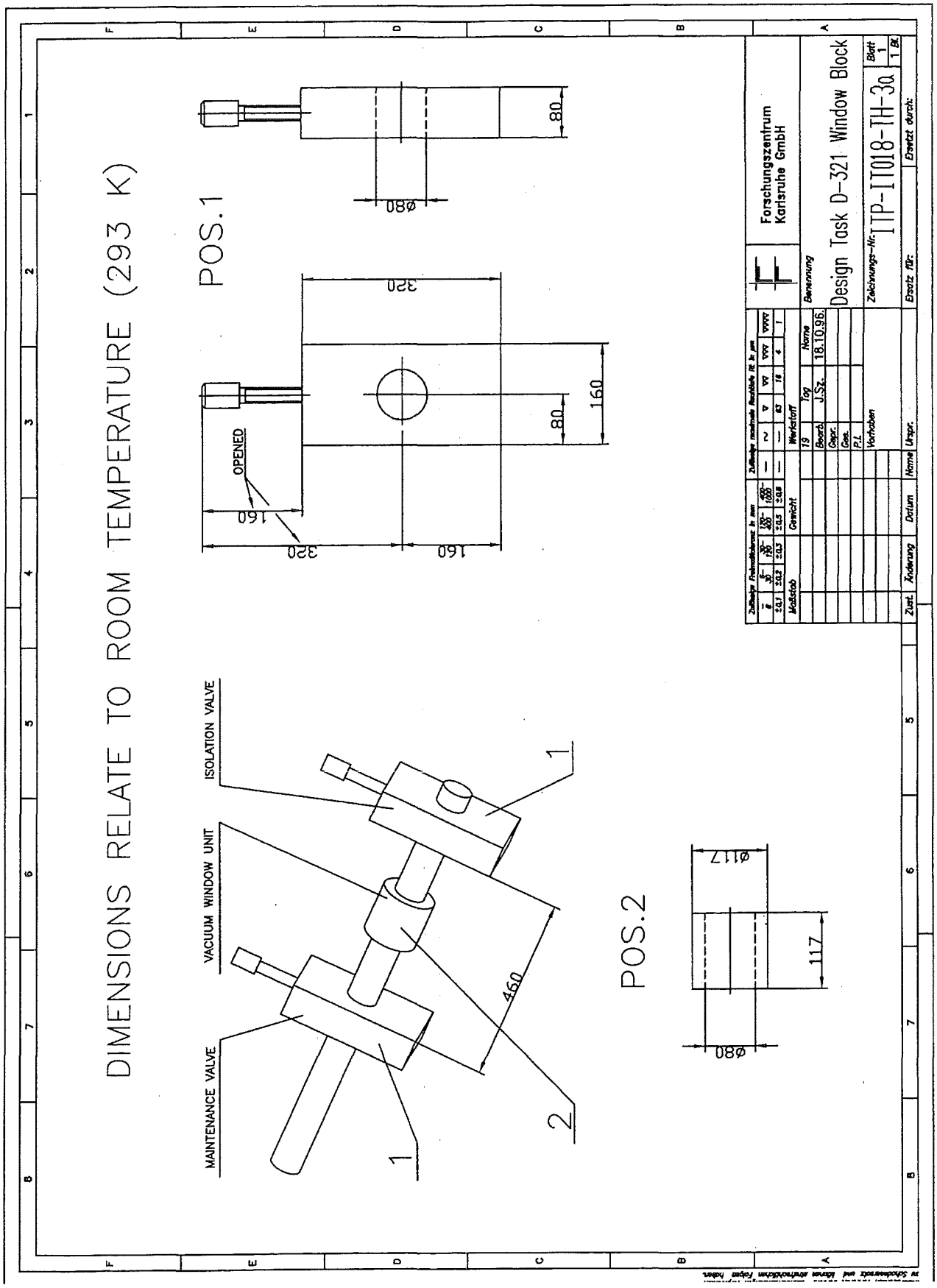

Fig. 5.2: Schematic drawing of the window assembly containing the vacuum window unit and the maintenance and isolation valves.

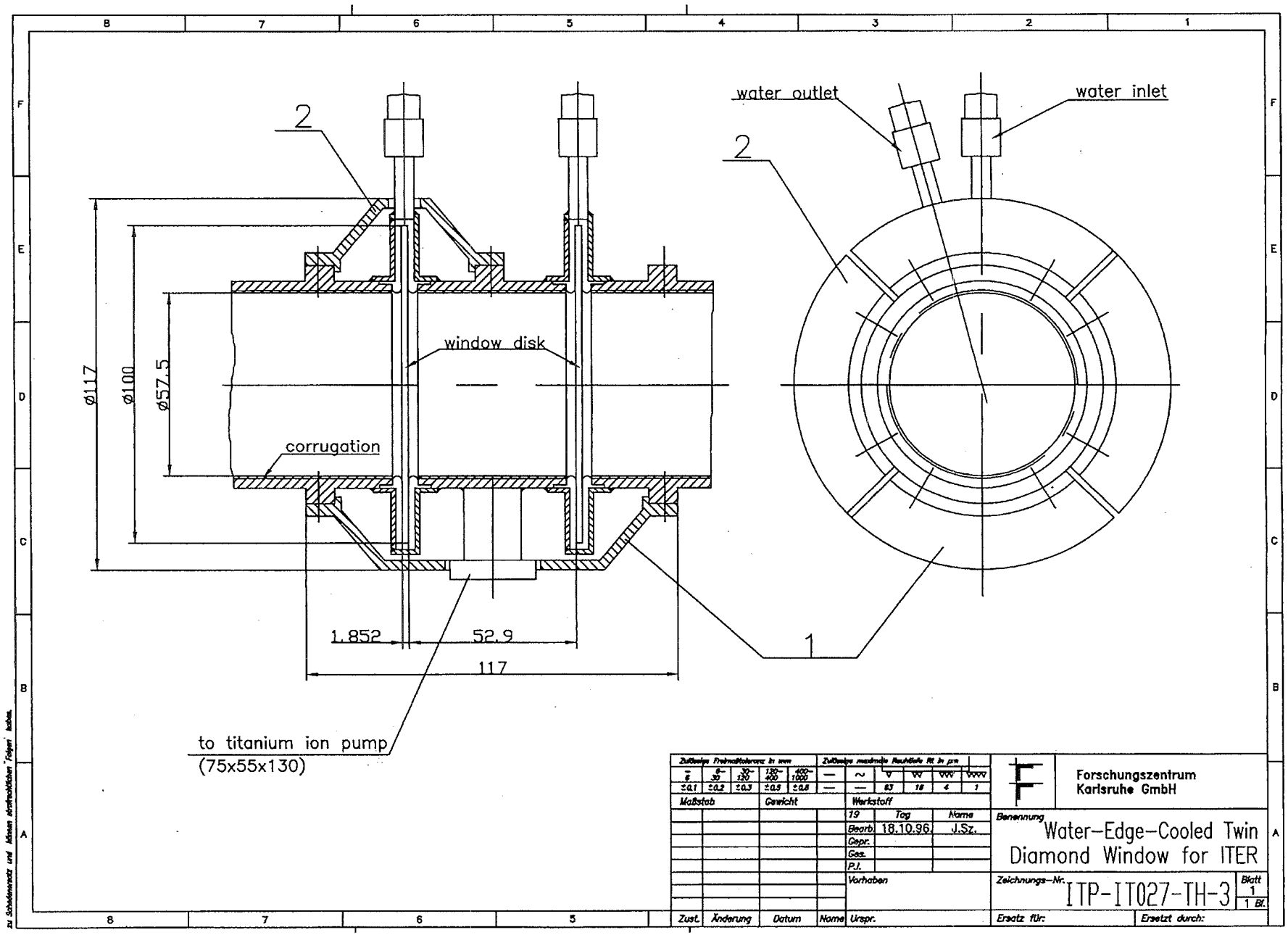

Fig. 5.3: Water-edge cooled, double-disk diamond window unit.

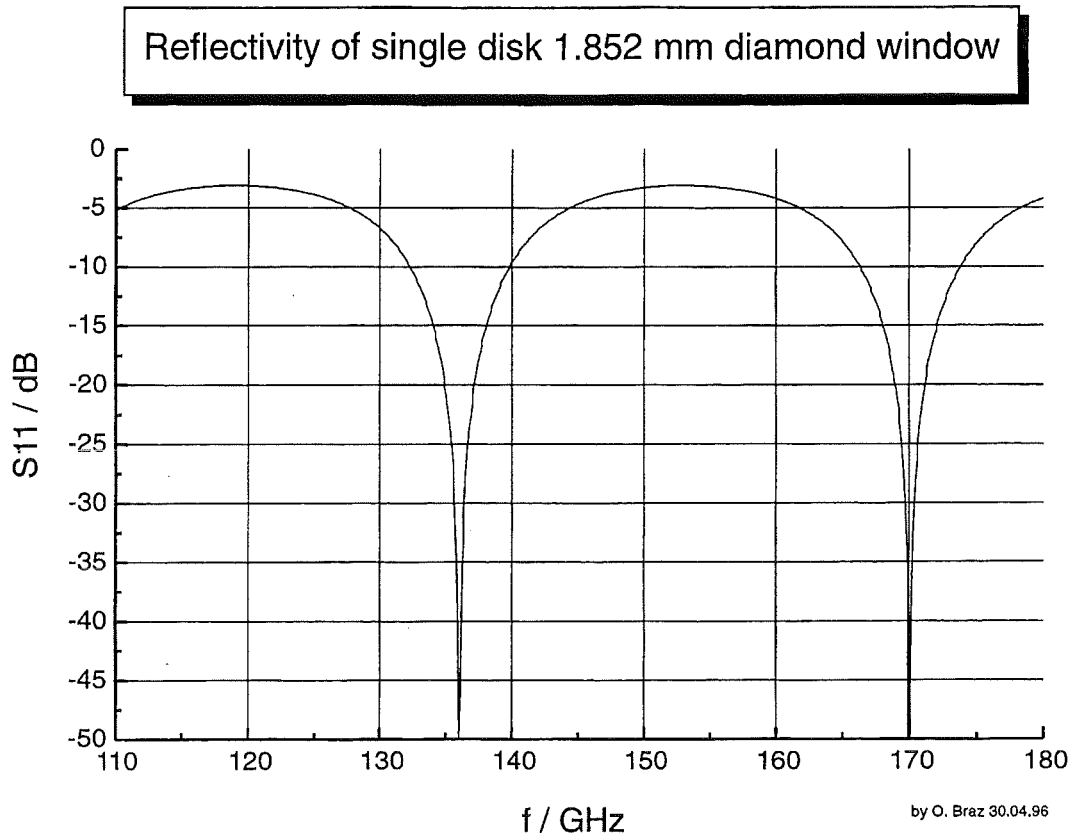

Fig. 5.4: Reflectivity of a single disk diamond window (disk thickness d = 1.852 mm)

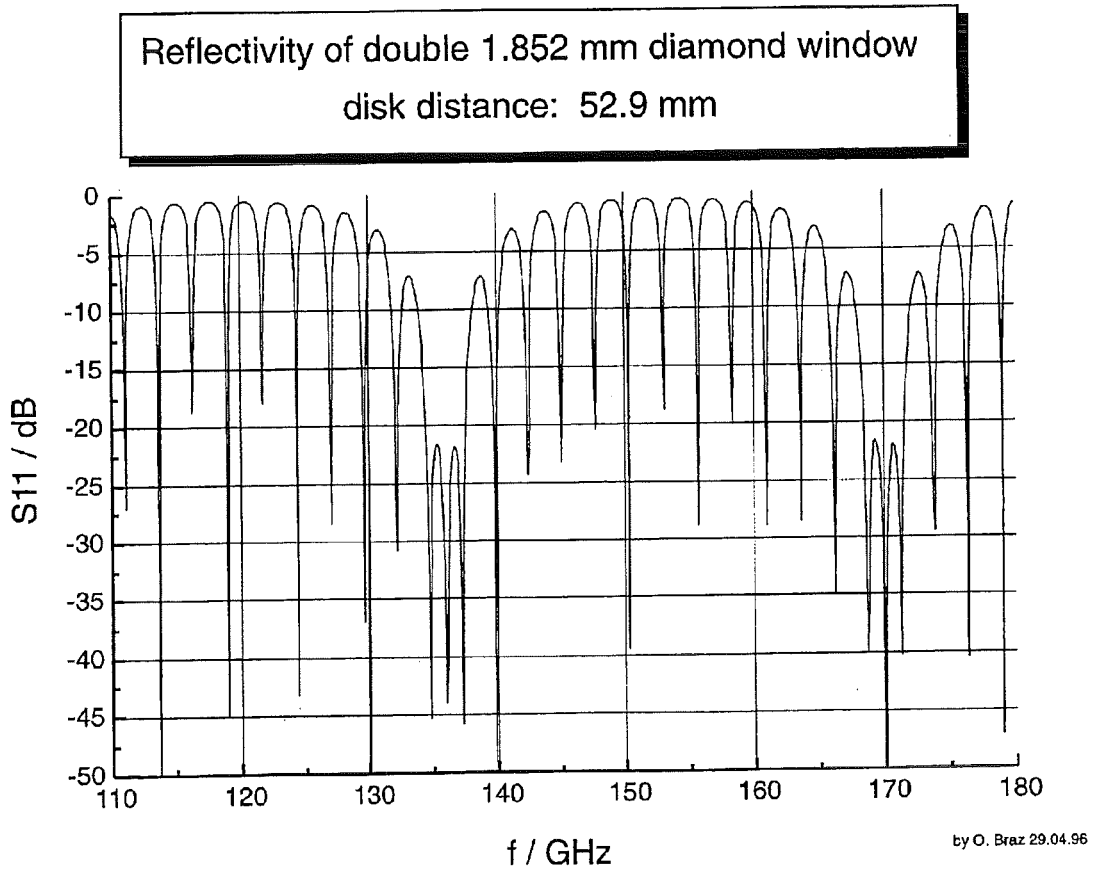

Fig. 5.5: Reflectivity of double-disk diamond window (disk thickness d = 1.852 mm, disk distance $l = 52.9 \text{ mm} = 30 \cdot \lambda$).

Through the use of a double disk window (Fig. 5.3), window failures can be easily detected (as on the JET LH and ICRH systems) even in the case that no arc detector with fiber optics light guides can be used in the nuclear environment. A very high vacuum ($\approx 10^{-7}$ Pa) can be achieved within the interspace between the two window disks. Since the total volume is small, vacuum pumping can be done with only one Vac-Ion pump. Any failure of either window is detectable as a pressure rise on the ion pump even in the case in which a lower case vacuum ($\approx 10^{-3}$ Pa) is present on the opposing surfaces. Bandwidth calculations show, that the disk distance should be e.g. 52.9 mm = 30 λ. The resulting bandwidth is 3.0 GHz which is somewhat broader than for a single-disk window (Figs. 5.4 and 5.5). Since the loss tangent and permittivity prove to be constant in the temperature range 200-360 K and because the thermal expansion of diamond is negligible, we have also constant reflection features of the diamond disks, so that there will be no problems of trapped power (no resonant cavity) between the two window disks. A double window is also good for lower tritium permeation.

The titanium ion getter pump should be a pump with 50 μA ion pump current employing a 5 kV/1mA power supply (as in the JET LH system).

6. Maintenance of Window Block and Safety

This section summarizes the general assumptions, classifications, guidelines and procedures for the maintenance of the window block.

The base assumptions for the mechanical design of the ECH system are:

First, the antenna is assembled and tested in the workshop, then it is installed inside the machine in less subparts as possible. Wave of the future seems to be to design a monolithic, self contained structure which can be inserted and removed from the port as a simple unit.

Second, the maintenance is done in the hot cell instead of inside the vessel. The design is optimized to simplify the assembly and disassembly of the system, rather than to replace or to repair in place small features.

Third, the port layout should be as close as possible to the standard solution to allow any different application and the use of the remote maintenance port as additional diagnostic ports.

In order to simplify the remote maintenance of the ECH system and to test it before installation in the port, the in-vessel transmission component chain will be assembled from three modules (see Fig. 1.1):

- Shield/blanket port plug,
- Mirror and waveguide port plug assembly,
- Window block assembly.

All three assemblies are safety importance class SIC-2 items (see Appendix I for the definition of terms). The first of these, the shield/blanket port plug, functions generally as all other shield/blanket modules. No ECH transmission components are physically attached to it. The mirror and waveguide port plug assembly contains the steerable optics and their actuation hardware. This will be designed to maximize access without extraction of the assembly from the port.

The window block assembly is accessible from the pit and will be designed to maximize hands-on maintenance. The windows are generally regarded as the most sensitive component of the system. The window block is located at the cryostat and is easily accessable from the pit. Due to the low dose rate, < 20 μS/hr, in this area [21], this assembly can be fully hands-on maintained. All remaining components are ex-vessel and outside of the second containment boundary. They are therefore class SCI-4 and will not be discussed further.

The system has been designed with sufficient extra capacity and redundancy so that the total system performance can be maintained even as elements of the system degrade. Maintenance will only be performed on the system when the system performance has dropped below the minimum specification (80% of the power available 100% of the time) [22].

6.1 Safety Importance Classification of Window Block

The safety importance classes (SIC) are defined in Appendix I. The in-vessel ECH transmission equipment from the vacuum vessel up to, and including the windows and isolation valves are part of the first and second containment barriers and belong to safety importance class SIC-2. The maintenance valves and associated interlocks and controls are redundant parts of the first confinement barrier and assist in lowering the frequency of loss of vacuum accidents. They are SIC-3. A schematic of the in-vessel system is shown in Figure 6.1. All ex-vessel components are SIC-4 (serve no safety functions) and will not be discussed further.

Two confinement boundaries are required for safety. One boundary must provide "absolute containment" in the sense of uninterrupted physical tritium barrier.

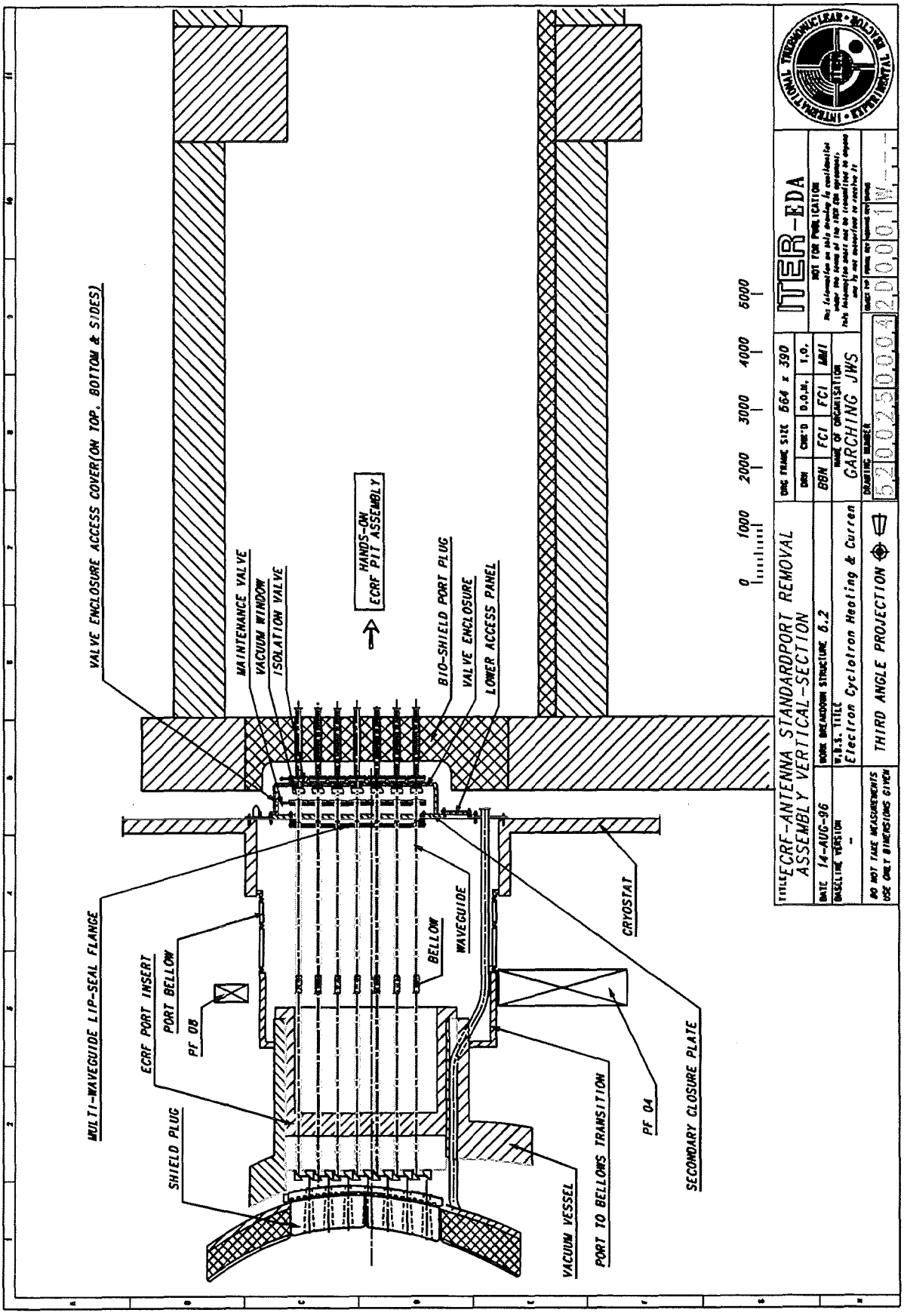

Fig. 6.1: Schematic drawing of removal - complete ECH-antenna assembly / vertical section.

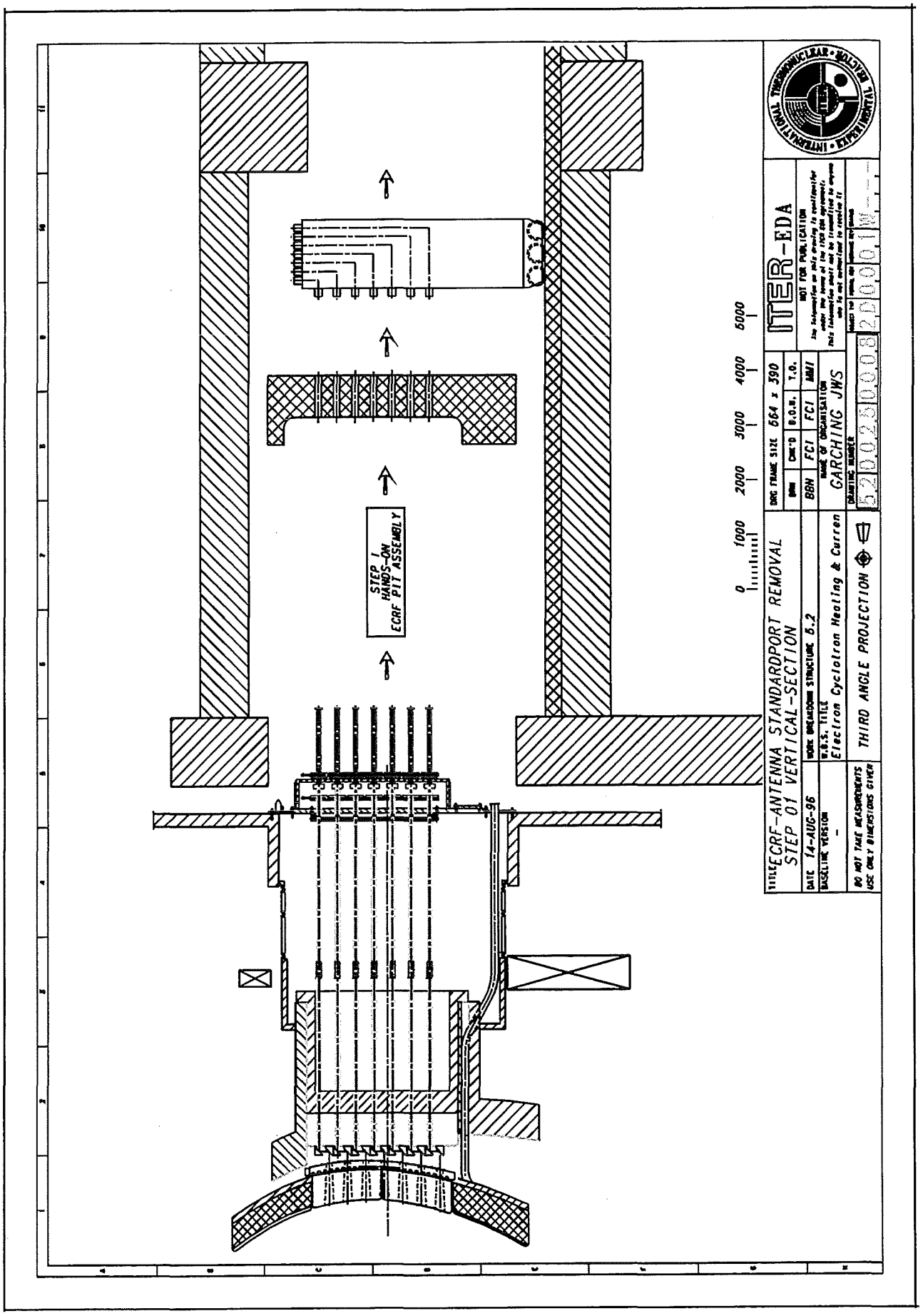

Fig. 6.2: Schematic drawing of removal step 1 / vertical section.

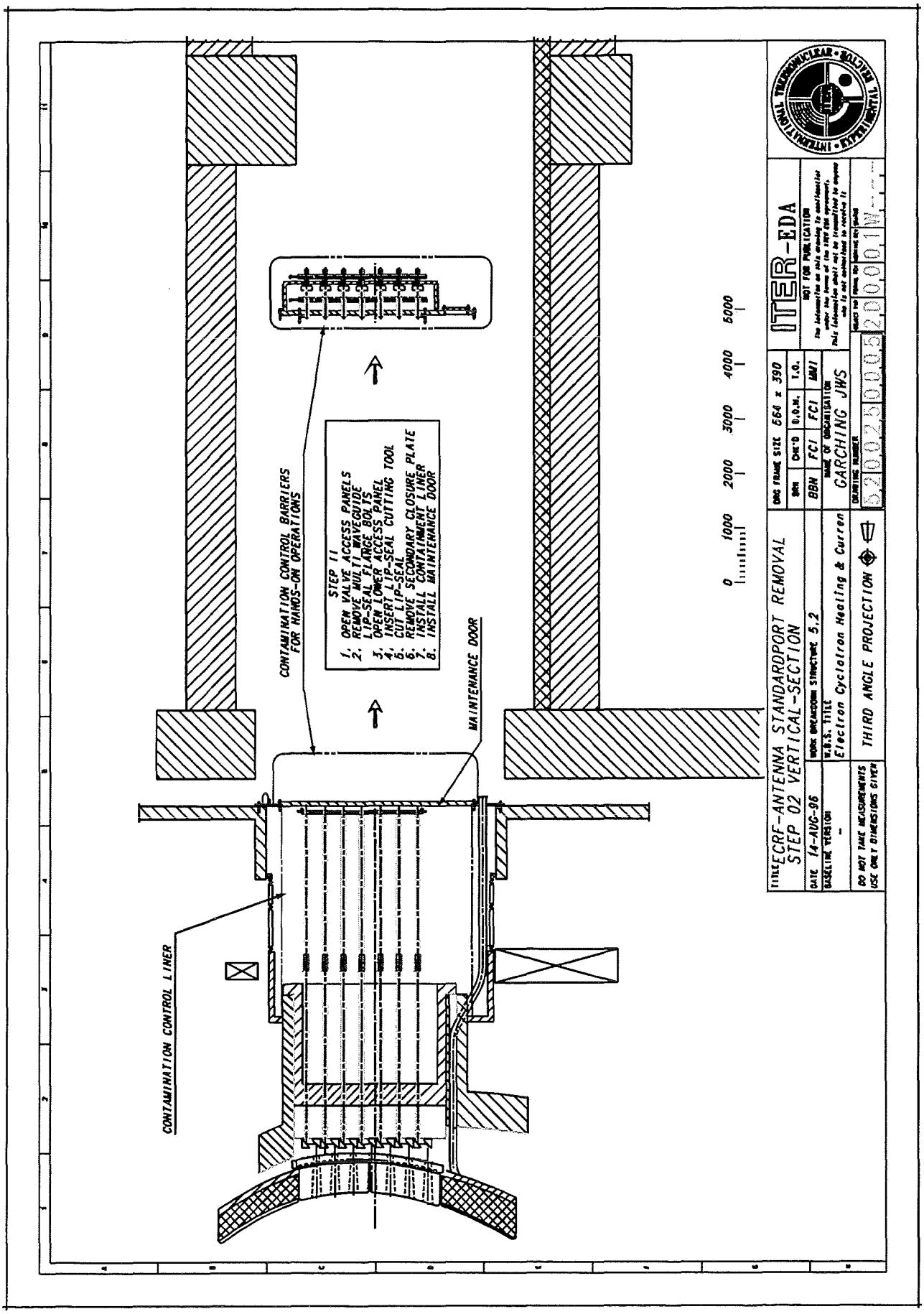

Fig. 6.3: Schematic drawing of removal step 2 / vertical section.

6.2 Maintenance Scheme and Procedure

The window block is located very close to the cryostat (Figs. 1.1 and 1.2) within the bioshield. Waveguides are passing the bioshield. Double containment of the tritated volume is required. Primary containment is made at the end of the port extension which avoids the necessity of large diameter 0.5 MPa bellows. The cryostat bellows belong to the secondary confinement and thus only have to be proper for 0.2 MPa accidental over pressure events. Standard bellows design can be used and we have no extension of the primary vacuum. Primary vacuum is carried through the waveguides to the windows. So, present containment strategy calls for the use of the window for absolute containment (primary containment) and a fast-acting isolation valve as the waveguide secondary containment. The port secondary containment is formed by the cryostat and a small volume, surrounding the maintenance valve and the window. Remote maintenance is feasible - several methods are being developed and are under analysis.

The vacuum windows and the safety valves are located in the port volume close to the cryostat flange, this room is used for leak test. The valves are gate type with metal gasket and the shaft sealed by a metal bellow. The gate is moved by a screw jack driven with tool which is connected through the service access in the cryostat flange. The valves and the vacuum window are maintained or replaced after removal of the cryostat flange, the waveguide being not continuous through that barrier. Permanent motors could be possible in the valves, if they can survive the radiation. In this case they are wired up to the plugs behind the service access. Their operation would require the opening of this small flange and the connection of the electrical power to the appropriate plug.

Failed components will be remotely replaced with spare units conducted at atmospheric pressure (dry N_2), maintaining at least one containment barrier at all times (maintenance valve) to avoid the spread of tritium and activated dust (Figs. 6.1 - 6.3). Maintenance of port and in-vessel components is performed using transfer casks that dock with the cell/double seal door at the ECH-port (mid-plane). The transfer casks contain remote handling systems and tools necessary to perform all (dis) assembly tasks. Failed components are transferred to the hot cell facility for repair or waste processing. The window block design must insure sufficient space for the insertion and removal of the necessary tools. All liquid and gas pressure bearing joints must be capable of being leak detected by remote means. Mechanical guides should be provided to aide final positioning and alignment and to protect adjacent components from the damage due to collisions.

7. Edge-Cooled Single-Disk Sapphire Cryo-Window at 30 K

This much more complicated torus window option is kept as a back-up solution. Lowering the temperature of a sapphire window disk to T = 20-30 K results in a strong reduction of tanδ and permits operation in the range of maximum thermal conductivity (Fig. 7.1) [17]. The power transmittance capability increases at least by a factor of 5.6, allowing even 2 MW windows at 170 GHz to be operated with the HE_{11} mode. However, in contrast to liquid nitrogen cooled windows, such windows always must be operated in an evacuated waveguide in order to avoid freezing.

For heat removal one can use a forced He-gas flow or, more simply, a liquid helium cooled thermal copper anchor around the window disk [7,8]. Another possibility is the use of nucleate (bubble) boiling liquid neon (neon bath) [6]. Neon could be simply liquefied by making use of an available flow of cold He gas.

The FZK LNe window design is based on a single circular disk of 140 mm diameter and 1.74 mm thickness ($6 \bullet \lambda/2$) in a short cylindrical waveguide structure of about 90 mm diameter. The

microwave energy absorbed in the window disk is removed by bubble boiling liquid neon at atmospheric pressure (27.15 K) in a rim around the edge of the disk.

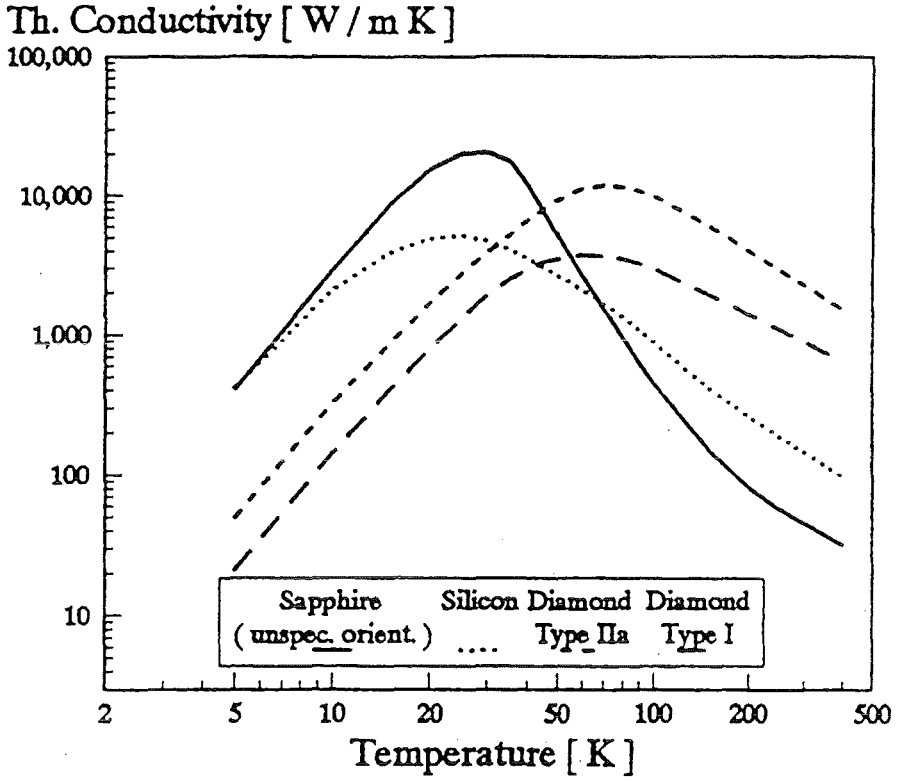

Fig. 7.1: Thermal conductivity of sapphire, silicon and diamond [17].

7.1. Thermal Finite Element Calculations

Optimization and design calculations on a liquid neon edge cooled single disk sapphire window for high-power CW millimeter waves in the frequency range between 140 and 220 GHz have been performed using the finite element code ABAQUS supported by the pre-processor code FEMGEN for preparation of the discretization mesh.

Using the measured power absorption factor of $\tan\delta = 1.48 \cdot 10^{-11}$ (f/GHz) $\cdot$ $(T/K)^2$ (pessimistic value) (Fig. 7.2) for Ti-doped sapphire and the relatively low value ($\approx$1500 W/mK) for the thermal conductivity, recently measured at CEA Cadarache for HEMEX grade quality (Fig. 7.3) [23], the maximum calculated CW power transmission for a Gaussian / HE_{11}-power distribution is 2.8 MW, 2.3 MW and 1.8 MW at 140 GHz, 170 GHz and 220 GHz, respectively. The numerical results are summarized in Figure 7.4 and Table VI. These calculations used a heat transfer coefficient of 1.5 kW/m^{2}K.

That means, that lowering the operational temperature from 77 K to about 30 K increases the power capability by a factor of about 5.6, allowing even 2 MW windows at 170 GHz to be operated with the HE_{11} mode. However, in contrast to liquid nitrogen cooled windows, liquid neon cooled windows always must be installed in an evacuated waveguide.

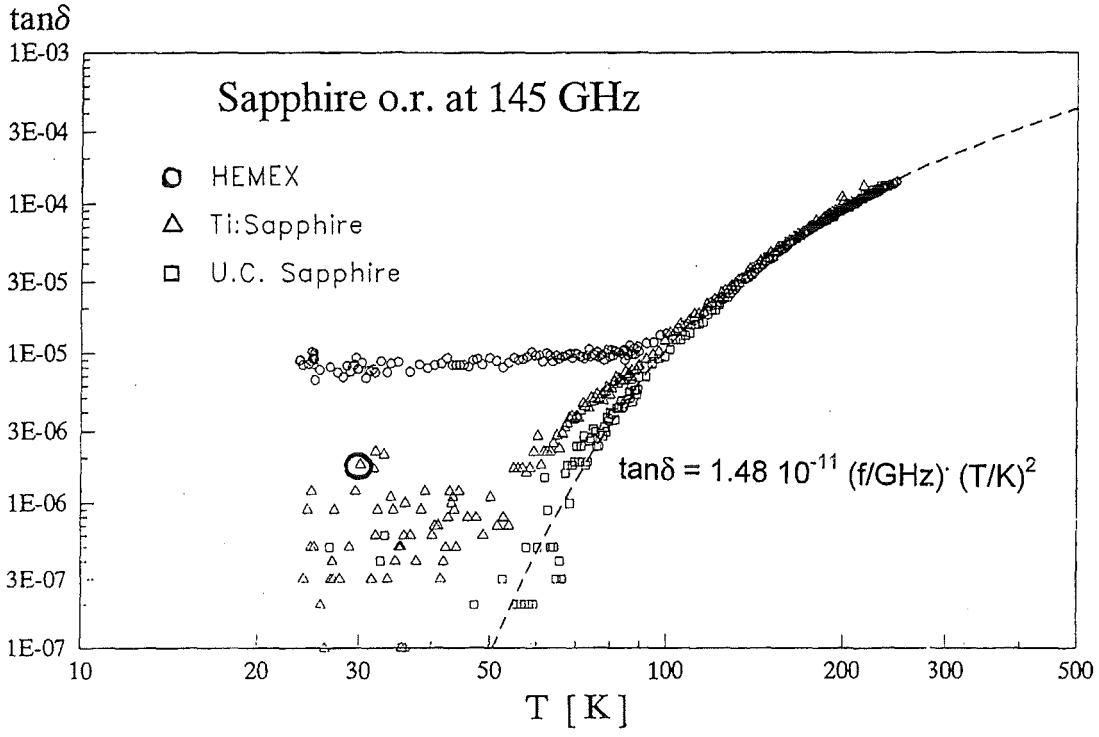

Fig. 7.2: Temperature dependence of dielectric loss of various sapphire grades.

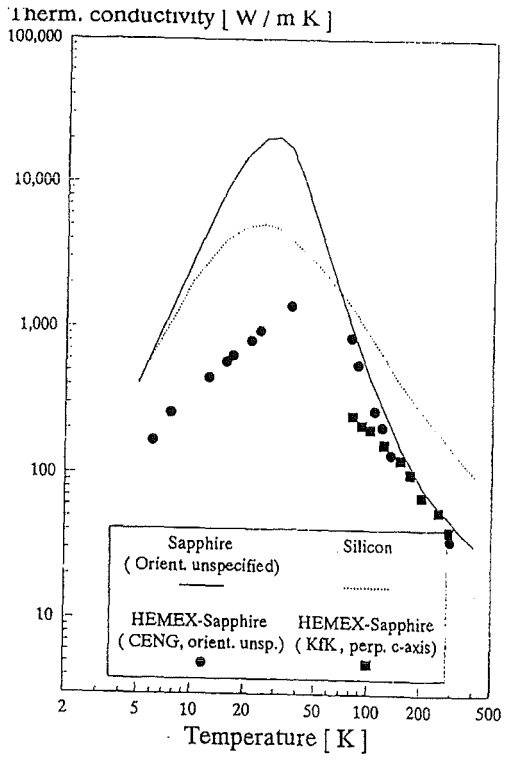

Fig. 7.3: Recommended thermal conductivity data [17] compared with measurements [21].

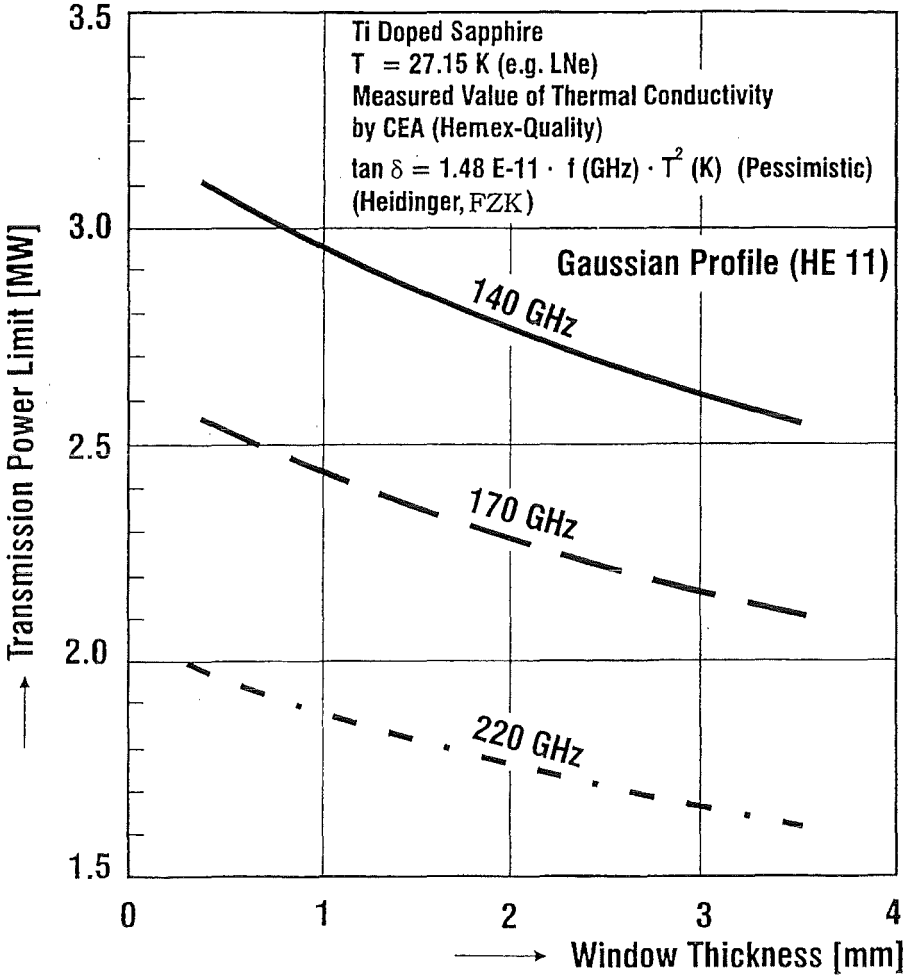

Fig. 7.4: Maximum transmission power as a function of window thickness.

The following Table VI summarizes numerical results of computations on the thermal window behavior for different frequencies and power using a Gaussian/HE_{11}-power distribution.

f (GHz)	thickness d (mm)	P (MW)	T_{max}/T_{min} (K)	$Q_{absorbed}$ (W)
118	2.09	1.0 (0.5)	33 (30) / 27	58 (29)
140	1.74	1.0	33 / 27	55
140	1.74	2.6 (max.)	48 / 30	241
170	1.72	1.0	34 / 29	67
170	1.72	2.1 (max.)	47 / 30	231

Table VI: Results of thermal finite element calculations for various LNe-cooled sapphire windows.

7.2 Finite Element Calculations on Stresses

Finite element calculations on stress distribution and overpressure have been also performed using the ABAQUS code supported by FEMGEN for preparation of the discretization mesh.

-step 1: cooling down of the window to 77 K with a full pressure difference of $\Delta p = 0.5$ MPa (poisson coefficient of steel = 0.3 was used).
-step 2: superposition of CW-gyrotron power distribution

The main stress in the window (260 MPa) is at the brazing collar due to the pressure difference. Since the measured bending tensile strength of HEMEX sapphire is around 500 MPa and the compressive strength is approximately 2800 MPa all stresses are below the admissible limits. However, for an industrial design, also the stress due to the brazing/bonding has to be taken into account, that strongly depends on the design of the brazing collar.

7.3 Thermal Radiation Load of Cryo-Window

The ohmic losses of high-power mm-waves heat up the transmission line components as e.g. mirrors of the miter bends and waveguide walls. The operation temperature of mirrors will be around 200 °C, the waveguide temperature will be lower.

Integration of Planck's radiation law yields for the total irradiated power I of thermal radiation the well-known Stefan-Boltzmann law:

$$I = \varepsilon\sigma T^4$$

where T is the absolute temperature in Kelvin,

$$\sigma = 2\pi^5 k^4/(15c^2h^3) = 5.67 \cdot 10^{-8}\ W/m^2K^2$$

and

$$\varepsilon(\text{emissivity}) = \alpha(\text{absorptivity}) \leq 1\,.$$

This formula shows, that at 200 °C (100°C) the total power radiated by a metal plate with 80 mm diameter cannot be larger than 14.3 W (5.5 W). Since the radiative heat flux from the fusion plasma propagating optically through the blanket plug, two miter bends and about 6.7 m straight waveguide is estimated to be approximately 5 W/dm^2, the total thermal radiation power reaching the window disk from up- and down- stream components will be lower than 15 - 20 W.
The wavelength at the maximum of the power distribution is described by Wien's displacement law:

$$\lambda_{max} \cdot T = \text{const} = 2.9 \cdot 10^{-3}\ m\ K.$$

This relation gives at the temperatures 273 K, 373 K and 473 K the wavelength of maximum power at 10.6 μm, 7.8 μm and 6.1 μm, respectively. Figure 7.5 shows the transmittance, reflectance and absorption coefficients of sapphire. The absorption at 6 - 8 μm is very high, so that we assume $\alpha = 1$ and therefore the upper limit of the absorbed thermal radiation power is 15 - 20 W. Therefore the total cooling capacity required for one LNe-edge-cooled sapphire window disk amounts to approximately 90 W (10 W intrinsic, 65 W absorbed mm-wave power, 15 W radiative load).

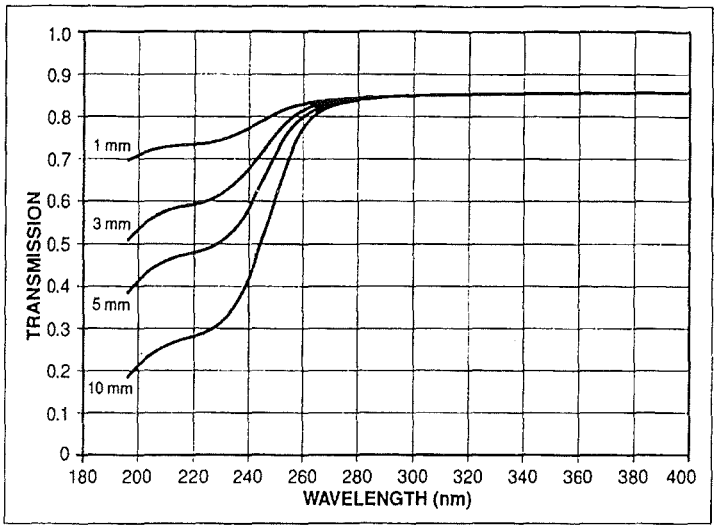

Ultraviolet Transmission for VUV Grade Sapphire as a Function of Thickness

CRYSTAL PRODUCTS

Union Carbide Chemicals and Plastics Co. Inc.
Industrial Chemical Division,
Crystal Products Group

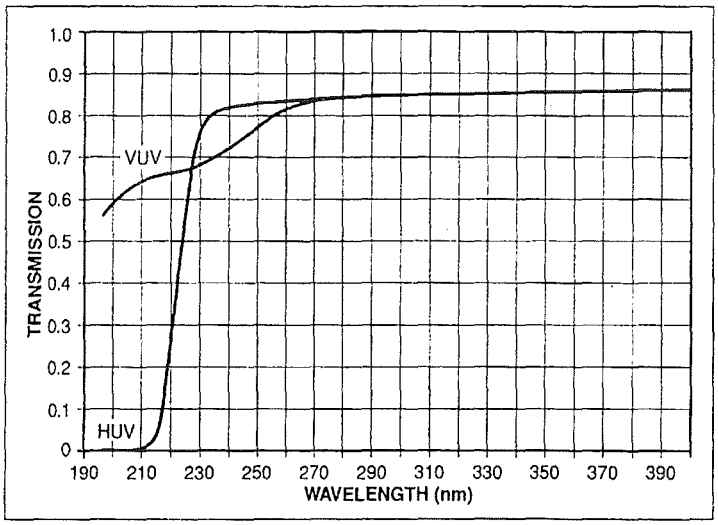

Ultraviolet Transmission for VUV Grade and HUV Grade Sapphire as a Function Wavelength

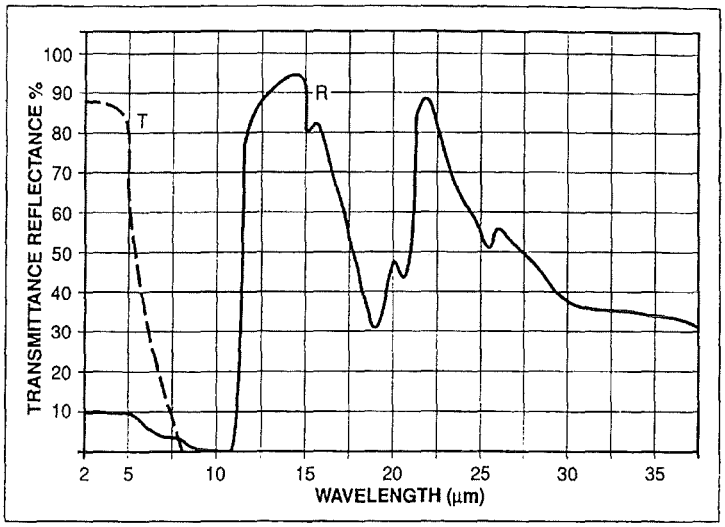

Transmission and Refectance of Sapphire in the Infrared[10]

Absorption Coefficient of Solid Sapphire as a Function of Wavelength for Various Temperatures. Data for the Curve Corresponding to 2020°C were Obtained by Heating the Samples with Flames; a Furnace was Used for the Remainder of the Data[12]

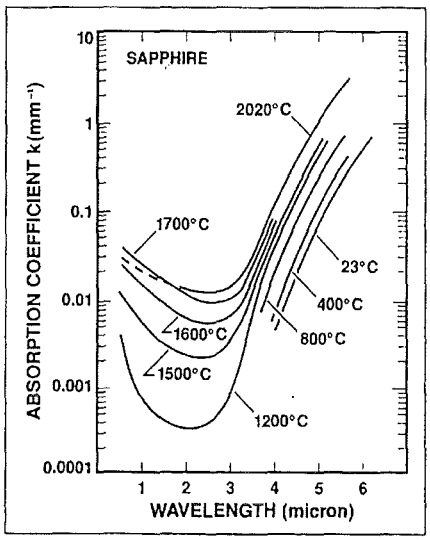

Fig. 7.5: Transmittance, reflectance and absorption coefficient of sapphire versus wavelength.

7.4 Scheme of Torus Window Array

The scheme of a model torus window array employing LNe-edge-cooled sapphire disks is presented in Figure 7.6. Several window units use the same isolation vacuum and common neon liquifiers and neon gas buffers. LN_2 cryo-trapping in a pumping waveguide cold trap on the torus side should pump the dust in the antenna waveguide. There is no danger of tritium condensation since this happens at lower temperature (20 K). The cryo-trap unit should include a heater for cleaning.

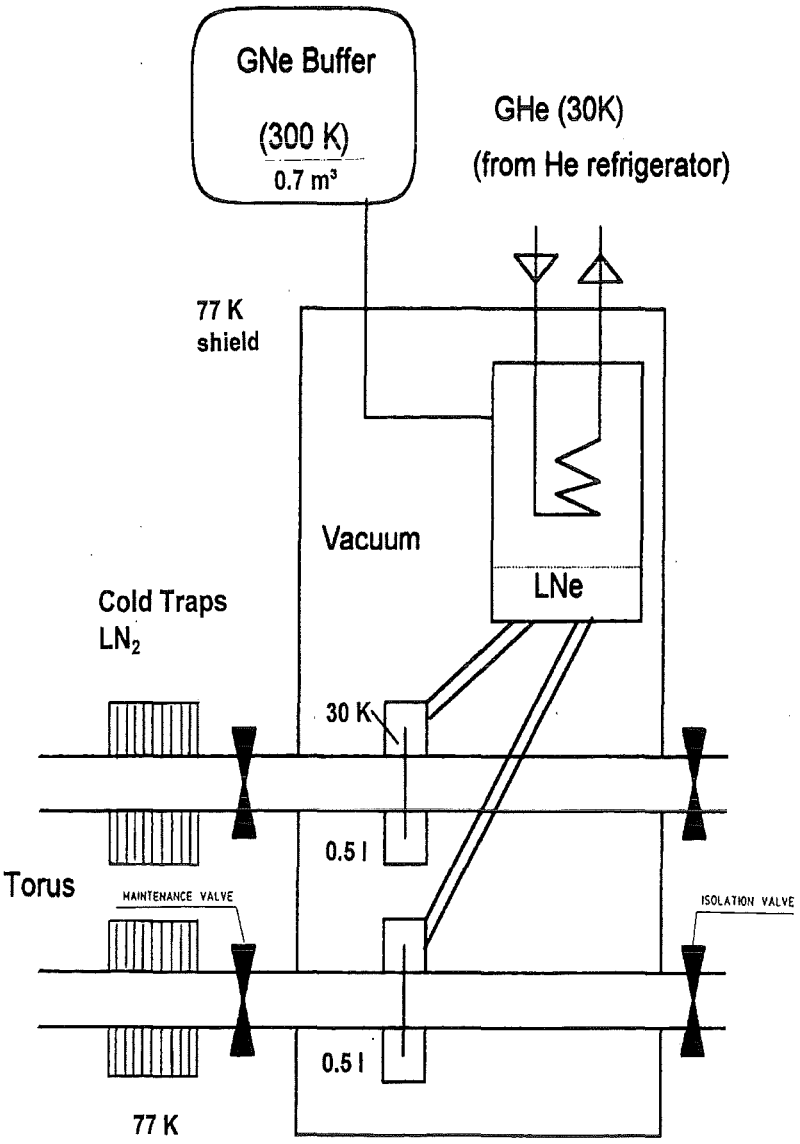

Fig. 7.6: Scheme of torus window array employing single-disk LNe-edge-cooled sapphire windows.

7.5 Experimental Validation of LNe-Cryo-Window Concept

At 0.5 MW, 118 GHz, 210 s operation the power absorbed by the window disk is 29 W and the maximum and minimum temperatures would be T_{max} = 30 K and T_{min} = 27 K, respectively (Tab. VI). The closed-cycle neon refrigeration system "Philips Cryogenerator PH 110" (refrigeration capacity: 150 W, Fig. 7.7) available at FZK Karlsruhe has been prepared to be used for first experimental tests on such a window system. However, since this cryo-generator is relatively bulky, an approximately 4 m long LNe-transmission line to the window cryostat (Fig. 7.8) was purchased from cryo-industries and is now available at FZK. Test runs of the cryogenerator and the transmission line were successful.

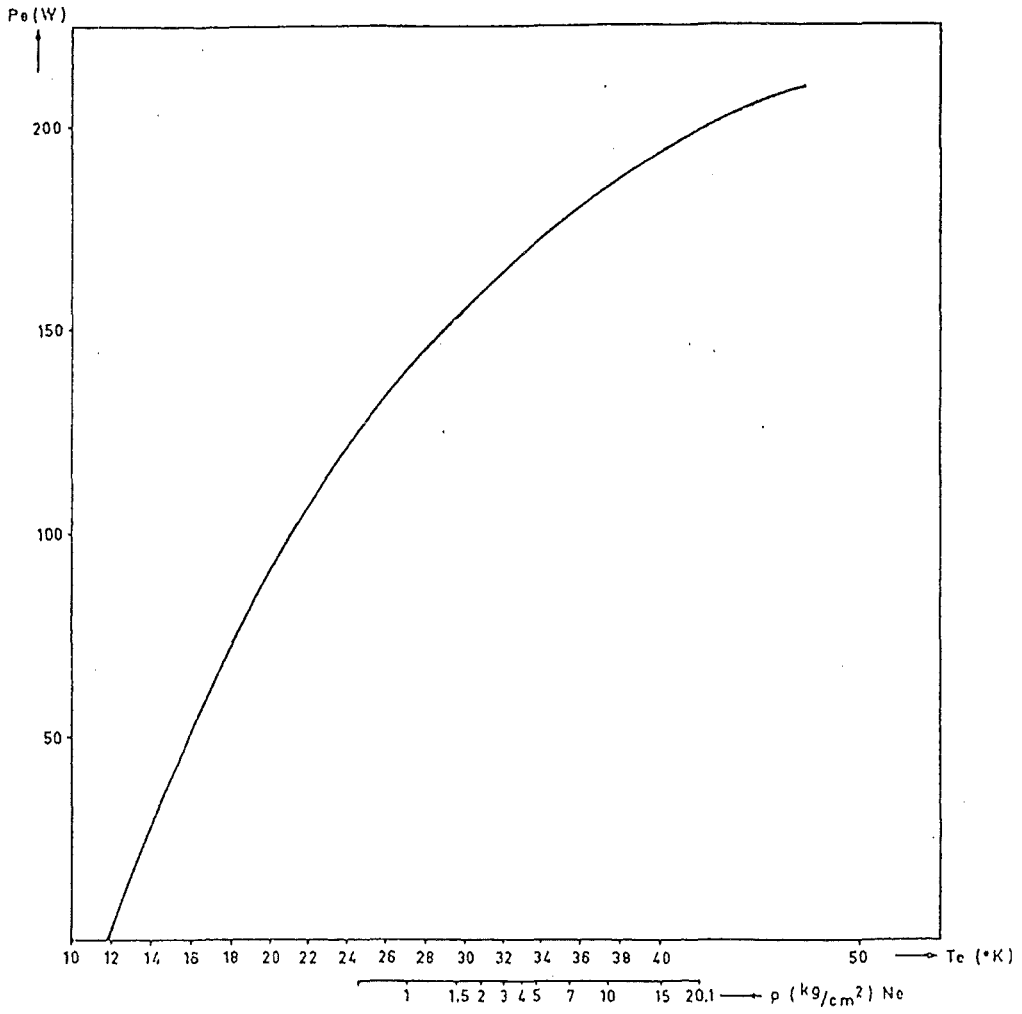

Fig. 7.7: Refrigeration capacity of Philips-Cryogenerator PPH 110.

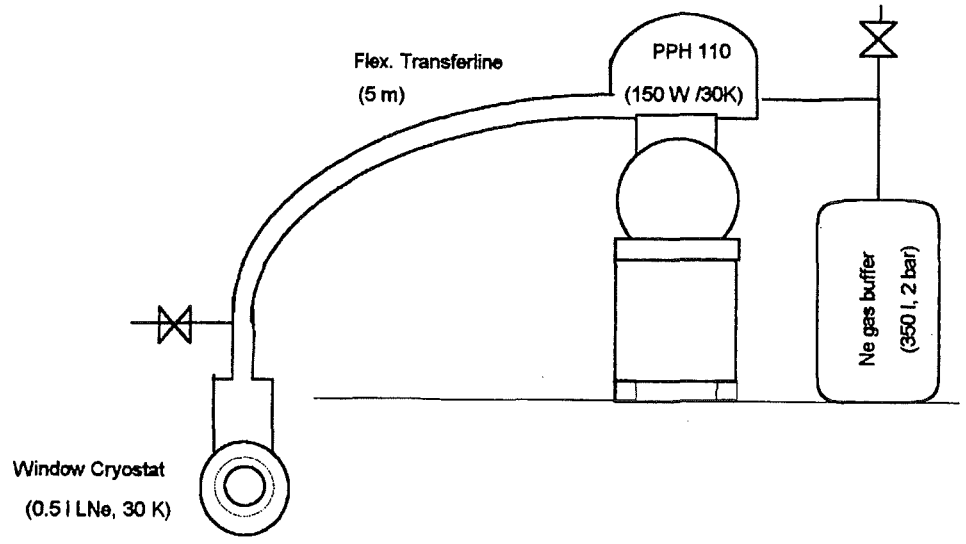

Refrigerator for the 30 K window

Fig. 7.8: Experimental setup for validation of LNe-cryo-window concept.

The window test could be performed at CEA Cadarache employing an improved version of the TTE 118 GHz gyrotron window assembly (Fig. 7.9) in an evacuated HE_{11} waveguide run (waveguide diameter = 63.5 mm). Special care has to be taken in order to minimize the static liquid neon consumption. Window cryostats with improved thermal isolation are presently under development at TTE. The diameter of the cryostat is 360 mm so that the window units must be staggered in order to keep the foreseen waveguide distance. The length of the cryogenic window unit would be about 250 mm.

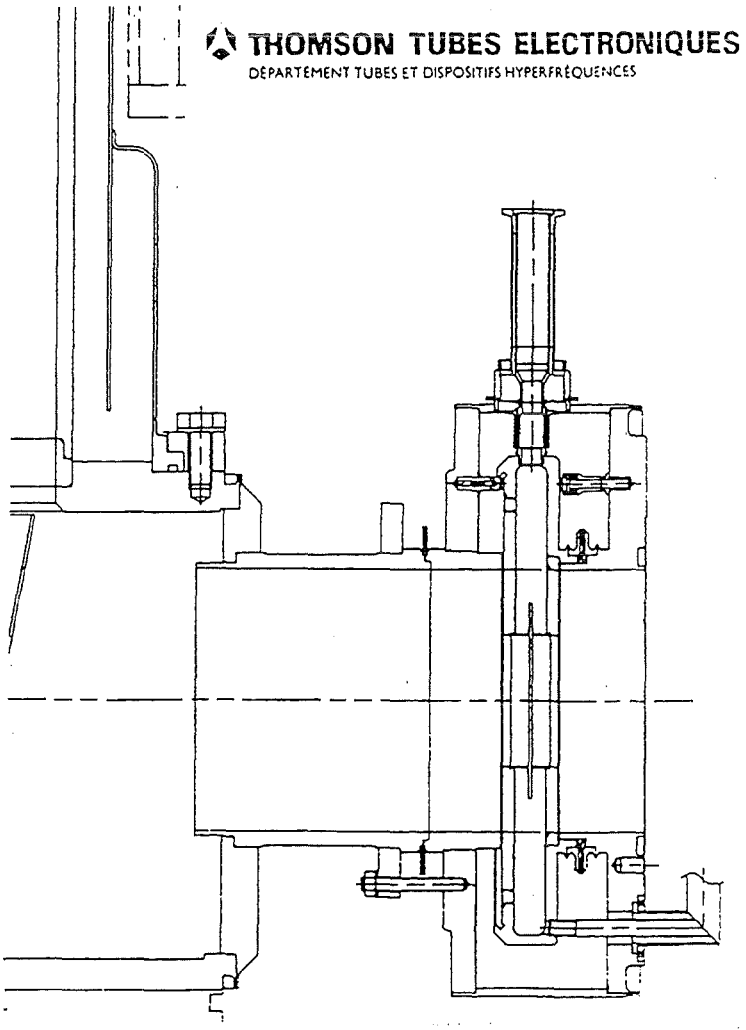

Fig. 7.9: Schematic drawing of the LN_2-edge-cooled single-disk sapphire window of the European quasi-continuous 210 s/500 kW 118 GHz gyrotron oscillator manufactured by TTE.

8. Broadband ECH Systems

A broadband transmission system is being developed for the start-up system. Initially, a system based on step-tunable gyrotrons is being developed which will allow operation at up to six frequencies in the band 90-140 GHz (three frequencies for each of the two independent start-up systems). As there is still concern regarding the reliability of mechanical components of the heating and current drive ECH system in a nuclear environment, a graded design strategy is being followed. An alternative which simplifies the system through the elimination of the movable components at the expense of overall system performance. The alternative make use of step-tunable gyrotrons and fixed, rather than steerable, optics. In this case a course frequency adjustment (e.g. three discrete frequencies) can be used to provide control of the deposition location within the plasma. Most capability is retained with the exception of off-axis current drive where the efficiency is reduced and the ability for accurate localization is lost.
A design study for two different step-tunable 1 MW gyrotrons using diamond windows have been performed at FZK (Table VII). The first operating at 131.4 GHz, 150.7 GHz and 170 GHz could be used for heating and current drive applications, and the second, operating at 95.9 GHz, 114 GHz and 132 GHz, could be used for the start-up system. A proposal of the Japanese Home-Team for a tunable gyrotron for start-up considers a tube which operates at 86.1 GHz, 108.1 GHz and 129.9 GHz in the $TE_{19,5}$, $TE_{24,6}$ and $TE_{29,7}$ modes, respectively.

Pilot experiments at FZK using a 1 ms gyrotron with an improved quasi-optical mode converter, single-stage depressed collector and fused quartz glass window ($12 \cdot \lambda/2 = 6.58$ mm thickness) gave 1.0 MW (41 % efficiency) in the $TE_{19,5}$ mode at 117.9 GHz, 1.2 MW (45 % efficiency) in the $TE_{22,6}$ mode at 140 GHz and 1.1 MW (49 % efficiency) in the $TE_{25,7}$ mode at 162.2 GHz.

The ultimate solution for a broadband window is the Brewster angle window. The Brewster angle for reflection free broadband transmission through a PACVD-diamond disk ($\varepsilon_r = 5.665$) is given by

$$\theta_{Brewster} = \arctan\sqrt{\varepsilon_r} = 67.21°$$

Thus, an elliptical diamond disk for a Brewster window in a HE_{11} waveguide with 57.5 mm diameter must have approximately the dimensions 150 mm x 90 mm. Current PACVD capabilities allow to produce samples of up to 110 mm diameter and about 2mm thickness. Manufacturers claim that they also can produce high quality samples of up to 160 mm diameter in near future, so that such Brewster windows are becoming feasible. The schematic drawing in Figure 8.1 shows the orientation of the Brewster window plate with respect to the polarization of the incident beam.

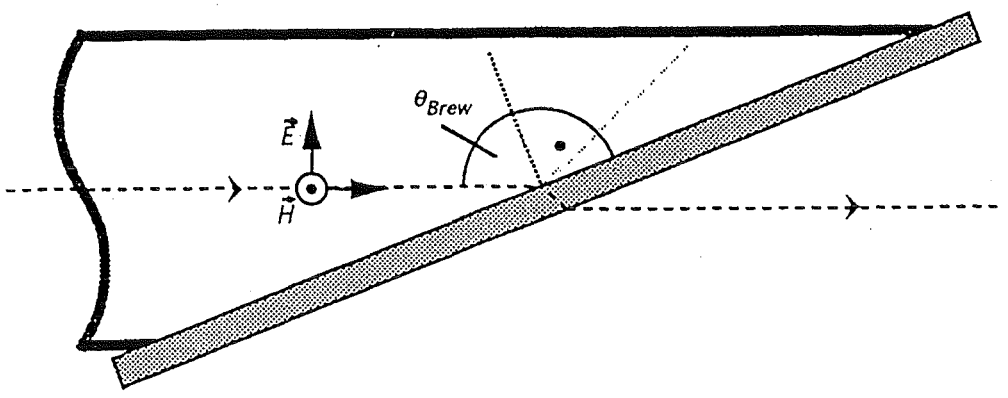

Fig. 8.1: Schematic drawing of a Brewster angle window.

Multi-Pass-Band Window for Step-Tunable Gyrotron

ITER Heating and Current Drive Gyrotron (CW)

Frequency	131.4 GHz	150.7 GHz	170 GHz
Mode	$TE_{25,6}$	$TE_{28,7}$	$TE_{31,8}$
Diamond Window Thickness 3.34 mm	7 λ / 2	8 λ / 2	9 λ / 2

ITER Start-Up Gyrotron (CW)

Frequency	95.9 GHz	114.0 GHz	132.0 GHz
Mode	$TE_{19,5}$	$TE_{22,6}$	$TE_{25,7}$
Diamond Window Thickness 3.31 mm	5 λ / 2	6 λ / 2	7 λ / 2

FZK Modelling Gyrotron (1 ms) with Single-Stage Depressed Collector

Frequency	117.9 GHz	140.1 GHz	162.2 GHz
Mode	$TE_{19,5}$	$TE_{22,6}$	$TE_{25,7}$
Fused Quartz Window Thickness 6.58 mm	10 λ / 2	12 λ / 2	14 λ / 2
Power (Eff.)	0.9 MW (36 %)	1.2 MW (45 %)	1.1 MW (39 %)

Table VII: Proposed multi-frequency ECH systems for H&CD and start-up on ITER and results of modelling experiments at FZK.

First experiments at FZK with a conventional cavity gyrotron (pulse duration 1 ms) equipped with a fused quartz Brewster window ($\theta_{Brewster}$ = 62.87°) gave approximately 1 MW output power for all operating mode series in the frequency range from 114 GHz to 166 GHz (frequency tuning in 3.7 GHz steps by variation of the magnetic field in the cavity). In Figure 8.2 the results achieved with the Brewster angle window are compared to those measured by employing a conventional single-disk window. This window (thickness d = 6.58 mm; 12 · $\lambda_n/2$) has been optimized to have low reflections at least for a few number of frequencies (Table VII).

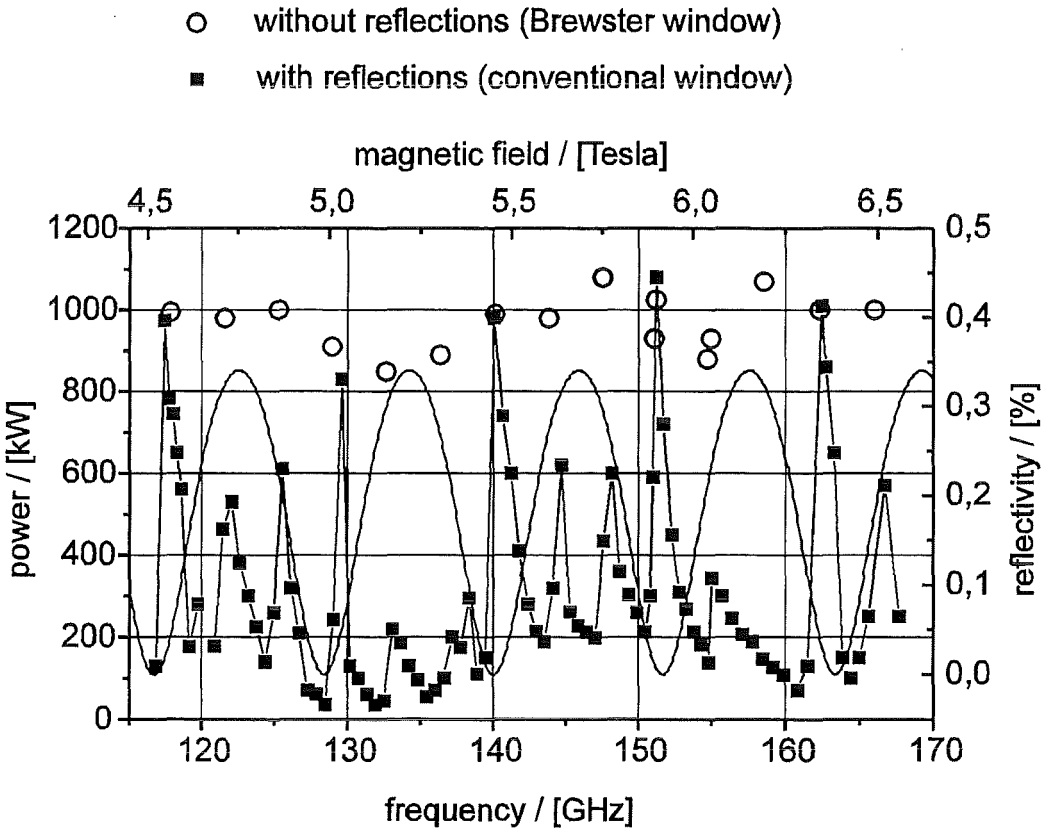

Fig. 8.2: Measured dependency of output power versus frequency for the two window concepts.

Appendix I: Safety Importance Classes

The following table has been extracted from the Section 4.1.2.4 of the ITER GDRD [22].

Safety Importance Classification

Safety Importance Class	Classification Rules
SIC-1	Components are classified in SIC-1 if the following rule applies: **Rule 1:** The component implements a safety function that is needed in normal operation or after occurrence of Category II (Likely) events and the failure of that safety function under such conditions leads to a release that exceeds the Category IV (Extremely Unlikely) limits.[1] (A design objective is to have no SIC-1 components in ITER.)
SIC-2	Components are classified in SIC-2 if any of the following three rules apply: **Rule 1:** The component implements a safety function that is needed after occurrence of Category III (Unlikely) or Category IV (Extremely Unlikely) events and the failure of that safety function under such conditions leads to a release that exceeds the Category IV (Extremely Unlikely) limits.[1] If the same safety function can be accomplished by another independent system, different from the one the component belongs to, then the component may be declassified to SIC-3. **Rule 2:** • The component is needed to provide an elevated (stack) release point for releases that can exceed 1/10th of the Category IV (Extremely Unlikely) limits.[2] **Rule 3:** • The failure of the component would degrade a safety function of a SIC-1 component..
SIC-3	Components are classified in SIC-3 if any of the following four rules apply: **Rule 1:** • The component implements a safety function whose failure could lead to a release that exceeds the Category II (Likely) limits[3] but is lower than the Category IV (Extremely Unlikely) limits. **Rule 2:** • The failure of the component would degrade a safety function of a SIC-2 component. . **Rule 3:** • The component implements a safety function needed to protect the facility personnel from radiological or toxicological hazards. **Rule 4:** • The component is needed for radiological monitoring of releases when they exceed the Category II limits (accident monitoring).
SIC-4	Not safety classified

References

[1] Makowski, M., 1996, Design of an electron cyclotron heating system for the ITER tokamak, Conf. Digest 21st International Conference on Infrared and Millimeter Waves, Berlin, AW1.

[2] Norajitra, P., Häfner, H.E., Thumm, M., 1995, Alternatives for edge cooled single disk windows with 1 MW transmission power, Conf. Digest 20th International Conference on Infrared and Millimeter Waves, Lake Buena Vista (Orlando), USA, pp. 475-476.

[3] Häfner, H.E., Norajitra, P., Müller, K., Thumm, M., 1994, Conceptual Design and Thermodynamics Study of Cryogenically Edge Cooled Windows for ECR Plasma Heating, 18th SOFT, Karlsruhe, Germany, Fus. Tech. Vol.1, pp. 505-508.

[4] Häfner, H.E., Bojarsky, E., Heckert, K., Norajitra, P., Reiser, H., 1994, Liquid nitrogen cooled window for high frequency plasma heating. Journal of Nuclear Materials, **212-215**, pp. 1035-1038.

[5] Häfner, H.E., Heckert, K., Norajitra, P., Vouriot, R., Hofmann, A., Münch, N., Nickel, H.-U., Thumm, M., Erckmann, V., 1994, Investigations of liquid nitrogen cooled windows for high power millimeter wave transmission, Conf. Digest 19th Int. Conf. on Infrared and Millimeter Waves, Sendai, JSAP Catalog No.: AP 941228, pp. 281-282.

[6] Thumm, M., Braz, O., Häfner, H.E., Heidinger, R., Möbius, A., Norajitra, P., Soudée, G., 1996, ITER ECH window development: Final report, ID No. T25, FZKA-Report No. 5808.

[7] Saitoh, Y., Itoh, K., Yoshiyuki, T., Ebisawa, K., Yokokura, K., Nagashima, T., Yamamoto, T., 1992, Cryogenic window for millimeter-wave transmission, Fusion Technology 1992, eds. C. Ferro, M. Gasparotto, H. Knoepfel (Elsevier Science Publishers B.V. 1992), pp. 632-636.

[8] Kasugai, A., Yokokura, K., Sakamoto, K., Tsuneoka, M., Yamamoto, T., Imai, T., Saito, Y., Ito, K. Yoshiyuki, T., Ebisawa, K., 1994, High power tests of the cryogenic window for millimeter wave. Conf. Digest 19th Int. Conf. on Infrared and Millimeter Waves, Sendai, JSAP Catalog No.: AP 941228, pp. 295-296.

[9] Pain, M., Berger-By, G., Capitain, J.J., Crenn, J.P., Smits, F., Tonon, G., 1992, The 110 GHz electron cyclotron heating and current drive system for Tore Supra, Proc. 8th Joint Workshop on Electron Cyclotron Emission and Electron Cyclotron Resonance Heating (EC-8), Gut Ising, Germany, Vol II, pp. 523-530.

[10] Fix, A.S., Sushilin, P.B., 1993, Calculation and experimental investigation of cryogenic window, Proc. 5th Russian-German Meeting on ECRH and Gyrotrons, Karlsruhe, pp. 389-392 and, 1994, Proc. 6th Russian-German Meeting on ECRH and Gyrotrons, Moscow, 1994, Vol. 2, pp. 244-247.

[11] Garin, P., Bon-Mardion, G., Pain, M., Heidinger, R., Thumm, M., Dubrovin, A., Giguet, É., Tran, C., 1995, Cryogenically cooled window: A new step toward gyrotron CW operation, Conf. Digest 20th International Conference on Infrared and Millimeter Waves, Lake Buena Vista (Orlando), USA, pp. 271-272.

[12] Shimozuma, T., Sato, M., Takita, Y., Kubo, S., Idei, H., Ohkubo, K., Watari, T., Morimoto, S., Tajima, K., 1995, Development of elongated vacuum windows for high power CW millimeter waves, Conf. Digest 20th International Conference on Infrared and Millimeter Waves, Lake Buena Vista (Orlando), USA, pp. 273-274.

[13] Moeller, C.P., Doane, J.L., DiMartino, M., 1994, A vacuum window for a 1 MW CW 110 GHz gyrotron, Conf. Digest 19th Int. Conf. on Infrared and Millimeter Waves, Sendai, Conf. Digest 19th Int. Conf. on Infrared and Millimeter Waves, Sendai, JSAP Catalog No.: AP 941228, 279-280.

[14] Heidinger, R., 1994, Dielectric property measurements on CVD diamond grades for advanced gyrotron windows, Conf. Digest 19th Int. Conf. on Infrared and Millimeter Waves, Sendai, JSAP Catalog No.: AP 941228, pp. 277-278.

[15] Heidinger, R., Link, G., 1995, The mm-wave absorption in sapphire and its description by the 2-phonon model, Conf. Digest 20th International Conference on Infrared and Millimeter Waves, Lake Buena Vista (Orlando), USA, pp. 16-17.

[16] Heidinger, R., 1994, Dielectric measurements on sapphire for electron wave systems, Journals of Nuclear Materials 212-215, pp. 1101-1106.

[17] Touloukain, et al., 1970, Thermophysical properties of matter, Vol.2, IFI/Plenum, New-York-Washington.

[18] Heidinger, R., Steinbock, L., 1996, The effect of x-ray irradiation on gyrotron window materials, Conf. Digest 21st International Conference on Infrared and Millimeter Waves, Berlin, AT8.

[19] Kerst, R. A., Swansiger, W. A., 1984, Journal of Nuclear Materials 122 & 123, 1499 - 1510.

[20] Riehm, M. P., Scheltzer, W. W., Thompson, D. A., 1986, CFFTP-G-86041-Report.

[21] Kripunov, V., Santoro, R. T., Iida, H., Discrete ordinates analysis of the nuclear performence of the ITER equatorial ports, NAG-11-11-13-96, November 1996.

[22] ITER General Design Requirements Document (GDRD), IDoMs Number S 10 GDRD 1 95-02-03 F1.

[23] Cadeau, M., Rouillon, H., Marcou, A., Novembre 1993, Mesures de conductivite thermique du saphir, CEA-CENG/DRFMC, Note SBT/CT/93-47.